Smart Prediction-Planning Algorithm for Connected and Autonomous Vehicle Based on Social Value Orientation

J Intel Connect Veh

Research Article

Smart prediction-planning algorithm for connected and autonomous vehicle based on social value orientation

Donglei Rong[1,2,3], Yuefeng Wu[4], Wenjun Du[5], Chengcheng Yang[1,6], Sheng Jin[1,2,7,✉], Min Xu[3], Fujian Wang[1,2]

Cite this article: Rong D L, Wu Y F, Du W J, et al. *J Intel Connect Veh* 2025, **8**(1): 9210053. https://doi.org/10.26599/JICV.2024.9210053

ABSTRACT: To improve the adaptability of Connected and Automated Vehicles (CAVs) in mixed traffic, this study proposes a prediction model training indicator that comprehensively considers drivers' Social Value Orientation (SVO) and planning goals. Active Influence Factor (AIF) is used as the goal to predict the future safety loss and consistency loss of CAVs. Second, an objective function based on SVO is constructed to understand the driver's characteristics to evaluate the safety, comfort, efficiency, and consistency of candidate trajectories. The results showed that integrating SVO and consistency functions can help ensure that CAVs drive under a more stable risk potential energy field. The prediction planning model that considers SVO can improve the reliability of the CAV output trajectory to a certain extent. The prediction planning under the AIF has better accuracy and stability of the output trajectory; however, it still has strong adaptability and superiority under different sensitivity parameters. The minimum and maximum standard deviations of our model are 0.78 and 0.78 m, respectively, whereas the minimum and maximum standard deviations of the comparative model reach 2.07 and 4.56 m, respectively. The minimum standard deviation of the other comparative model reaches 1.35 m, and the maximum standard deviation reaches 4.45 m.

KEYWORDS: Connected and Automated Vehicles (CAVs); Social Value Orientation (SVO); smart prediction planning; trajectory planning; numerical simulation

1 Introduction

In recent years, the integrated sensing, decision planning, and robust control of Connected and Automated Vehicles (CAVs) have promoted the rapid expansion of CAV application scenarios (Zhou et al., 2023). Limited by policy introduction, technical constraints, responsibility ethics, and other restrictive factors, CAVs and Human-Driven Vehicles (HDVs) will coexist for a long period of time in the future. Hence, the fundamental challenge that demands attention is the augmentation of decision-making capabilities in CAVs to emulate the cognitive processes observed in proficient human drivers (Bai et al., 2024; Dai et al., 2023).

Current scholarly discourse maintains a sanguine perspective on the holistic advancement of autonomous driving technology, coupled with the anticipation of a significant proliferation of CAVs within the transportation landscape. Research has extensively considered vehicle dynamic constraints (Jiang and Zhou, 2021) and proposed a situational awareness framework for trajectory planning in structured traffic environments (Dixit et al., 2018). Additionally, under high-speed conditions, CAVs are prone to approaching extreme operating conditions (Sazgar et al., 2018). Altche et al. (2017) established a virtual input double integrator that is based on extreme conditions and applied appropriate speed profiles to solve optimization problems. This approach constructs highly constrained trajectory corridors and optimal results under complex road conditions and vehicle operating conditions (Jeon et al., 2013; Wang et al., 2020). Research progress on CAVs in straight-line scenarios can be categorized into trends of intelligence (Dixit et al., 2018; Liu et al., 2018), collaboration (Tomas-gabarron et al., 2013; Richter et al., 2014), and dynamism (Michael and Stephen, 2016; Rong et al., 2024a). However, constrained by technological limitations, policy restrictions, and ethical considerations, the coexistence of CAVs and HDVs is highly likely to persist in the long term. Game theory serves as a vital approach for handling mixed traffic scenarios. Yu et al. (2023) proposed a multiagent dynamic game model that fully considers the states of surrounding vehicles to ensure accurate execution of lane-changing decisions. Yan et al. (2023) introduced a trajectory planning framework based on game theory, achieving dynamic evolution of planning from both lateral and longitudinal game perspectives. Zhou et al. (2019) extended

[1] Institute of Intelligent Transportation Systems, College of Civil Engineering and Architecture, Zhejiang University, Hangzhou 310058, China. [2] Center for Balance Architecture, Zhejiang University, Hangzhou 310058, China. [3] Department of Industrial and Systems Engineering, The Hong Kong Polytechnic University, Hong Kong 999077, China. [4] Xinchang Communications Investment Group Co., Ltd., Shaoxing 312500, China. [5] Zhejiang Institute of Communications Co., Ltd., Hangzhou 310030, China. [6] Department of Architecture and Civil Engineering, Chalmers University of Technology, Gothenburg 41296, Sweden. [7] Zhongyuan Institute, Zhejiang University, Zhengzhou 450000, China.

✉ Corresponding author. E-mail: jinsheng@zju.edu.cn

Received: June 3, 2024; Revised: August 23, 2024; Accepted: October 26, 2024

the game model to interactions among motor vehicles, nonmotor vehicles, and pedestrians, enabling CAVs to dynamically evaluate and respond to various uncertainties at complex intersections via a pipeline algorithm. In addition to game relationships, cooperation among CAVs is crucial. Therefore, Qiu and Du (2023) proposed an embedded mixed-integer nonlinear programming approach to realize cooperative planning of CAVs in mixed traffic, aiming for formation and efficient driving. Hubmann et al. (2017) defined human drivers' intentions as a partially observable Markov decision process, enabling CAVs to make judgments and responses in continuous state spaces. Cai et al. (2023) and Rong et al. (2024b) presented a hierarchical cooperative merging control strategy for entrance ramp merging in mixed traffic to optimize safe and flexible trajectories. In summary, existing research primarily utilizes game theory logic to infer and model feasible decision-making plans across different scenarios and entities, aiming to achieve low-risk and high-efficiency goals.

However, three core issues remain: (1) How can the quality of CAV candidate trajectories be effectively evaluated so that the output trajectory fully considers the subject factor CAV and the object factor HDV (Wang et al., 2023)? (2) How can the driver's Social Value Orientation (SVO) be fully evaluated to improve the accuracy of motion planning? (3) How to consider driver factors and planning goals in the prediction model so that the prediction results can be transformed from "prediction accuracy-oriented" to "planning goal-oriented" (Zhang et al., 2023)? Therefore, this study proposes a smart prediction planning algorithm for CAVs that is based on SVO. The main contributions of this study are as follows.

Contribution 1: Shifting from self-oriented to socially compatible planning. The traditional objective function focuses on safety, comfort, and efficiency and represents a self-oriented planning strategy. By introducing a consistency function, this strategy evolves into a socially compatible planning approach, enabling CAVs to consider potential inconveniences to other vehicles.

Contribution 2: Incorporation of Dynamic SVO (D-SVO). This study proposes a trajectory planning algorithm that accounts for D-SVO of drivers. This approach enhances planning effectiveness while maintaining robustness in various driving scenarios.

Contribution 3: Transition to smart prediction and planning. The concept of smart prediction and planning is introduced, shifting the focus from "prediction accuracy-oriented" to "optimization effect-oriented". This change leads to more efficient trajectory planning by prioritizing optimization over mere accuracy.

In addition to the introduction, this paper explains the research object, research questions, and research framework in Section 2. Second, three different prediction models are proposed in Section 3. The first is a future trajectory prediction model that is based on SVO. The second is the prediction of the future loss value via SVO, and the third is the prediction of the loss value impact index via SVO. In Section 4, an objective function based on SVO and consistency is constructed. Finally, the experimental results are analyzed for each innovation point in Section 5. The conclusions are presented in Section 6.

2 Problem description

2.1 Research subjects

CAVs and HDVs transmit basic safety messages from vehicles to vehicles. The research scenario is an ordinary road section. The main vehicle is set to CAV_{main}, the other CAV numbers are CAV_1, CAV_2, … , and the HDV numbers are HDV_1, HDV_2, … The trajectory data of the vehicle are $s = \{x, y, v, a, \theta, \kappa\}$, where x, y, v, a, θ, and κ are the lateral position, longitudinal position, speed, acceleration, deflection angle, and curvature, respectively.

In Fig. 1, the yellow vehicles represent CAVs, whereas the white vehicles depict HDVs. During predictive planning by CAVs, it is crucial to anticipate the trajectory of interacting HDVs and integrate this information into the CAV planning module. Assuming that the HDV drivers behave rationally, their predicted trajectory is considered normal. A prosocial driver tends to adopt a more conservative trajectory, whereas an aggressive driver may exhibit a more assertive trajectory.

2.2 Research problem

(1) How can the objectivity of evaluating the trajectory planning objective function for CAVs be enhanced, thereby ensuring that planning outcomes consistently satisfy driving requirements while prioritizing safety, comfort, and efficiency?

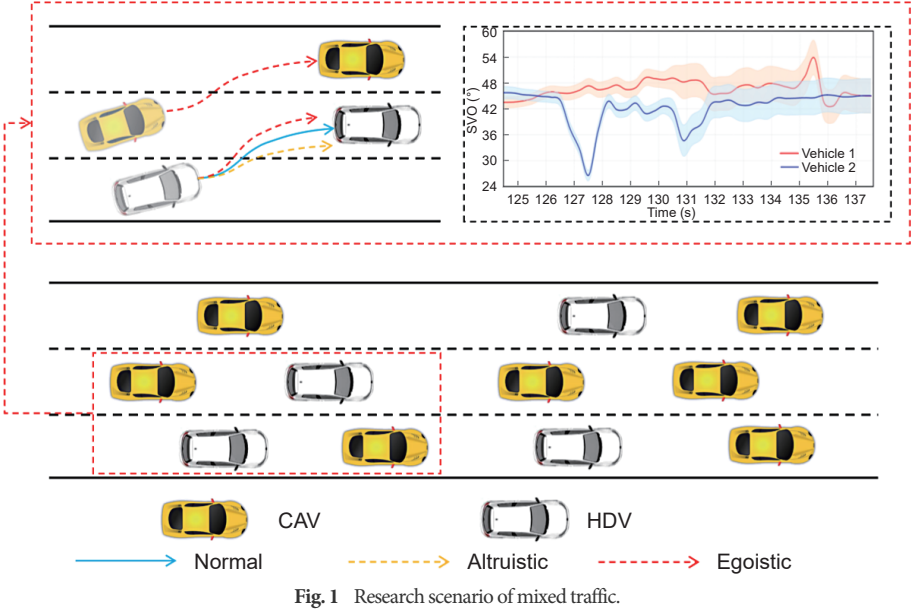

Fig. 1 Research scenario of mixed traffic.

(2) In what ways can the influence of HDVs driver characteristics on CAV prediction and planning be comprehensively assessed, enabling CAV trajectory planning results to better adapt to driving conditions within mixed traffic environments?

(3) How can the target requirements of CAV trajectory planning be effectively incorporated into the prediction process for surrounding vehicles, ensuring that prediction outcomes align more closely with the intended planning objectives?

2.3 Research framework

As illustrated in Fig. 2, the prediction module processes the SVO of nearby HDVs, along with the historical trajectory data of both HDVs and the CAV. The module employs three distinct training metrics to increase the prediction accuracy. The first metric, denoted minimum Average Displacement Error of trajectory as $\text{minADE}_{\text{traj}}$, minimizes the deviation between the predicted and actual future trajectories of HDVs. The second metric, minimum Root Squared Error of loss value ($\text{minRMSE}_{\text{loss}}$), focuses on reducing the deviation between the predicted and actual loss values of the CAV's candidate trajectories. The third metric, minimum Root Squared Error of AIF ($\text{minRMSE}_{\text{aif}}$), optimizes a planning-oriented training metric aimed at improving trajectory prediction. Following these predictions, the planning module evaluates each candidate trajectory via a loss function that incorporates safety, comfort, efficiency, and consistency. Additionally, the predicted future trajectories of HDVs are utilized in calculating the safety and consistency functions.

3 Prediction model

In the context of autonomous driving, SVO offers a systematic framework for modeling social dynamics between vehicles. Each vehicle is considered a rational agent, balancing its individual goals with broader objectives, such as safety and social cooperation. By incorporating SVO, we aim to represent the diverse motion-planning styles seen in real-world driving, where vehicles may not always prioritize the same outcomes. Each agent's trajectory is predicted on the basis of its SVO and historical data, influencing how it responds to the movements of other vehicles. A cooperative agent is more likely to predict trajectories that maintain safe distances and adjust speed to avoid conflicts, whereas a self-interested agent may prioritize reaching its destination efficiently, potentially at the expense of comfort or yielding to others. SVO plays a critical role in how agents balance self-interest with cooperative behavior in multiagent environments. The prediction model leverages SVO to anticipate how vehicles with different orientations—self-focused, cooperative, or competitive—will act on the basis of their observed behavior. Cooperative vehicles are expected to yield or maintain safe distances, whereas self-interested or competitive vehicles may prioritize efficiency (e.g., faster lane changes). Drawing from social preference theory, SVO helps predict how vehicles behave on the basis of their social orientation, increasing trajectory accuracy. SVO serves as input data for the prediction model and as a parameter for reconstructing the loss function.

F1 and F2 are used to predict the future trajectories of HDVs for the planning module. F1 relies solely on trajectory data, whereas F2 uses both trajectory data and SVO data as training inputs. F3 and F4, on the other hand, directly predict the loss value for each candidate trajectory in the planning module. F3 uses trajectory data and loss values as training inputs, whereas F4 incorporates trajectory data, loss values, and SVO data. As a result, F1 and F2 (or F3 and F4) can be compared to evaluate the impact of SVO. Additionally, F1 and F3 (or F2 and F4) can be analyzed to assess the differences in their outputs.

3.1 Trajectory prediction via SVO

As shown in Table 1, F1 and F2 are both prediction modules designed to forecast the future trajectories of HDVs. The key difference lies in their input sources: F1 relies solely on trajectory data, whereas F2 uses both trajectory data and SVO data as inputs. The evaluation metrics include Average Displacement Error (ADE), Final Displacement Error (FDE), and Miss Rate (MR).

This study uses Long Short-Term Memory (LSTM) to learn the interactive feature information of interactive vehicles (referred to

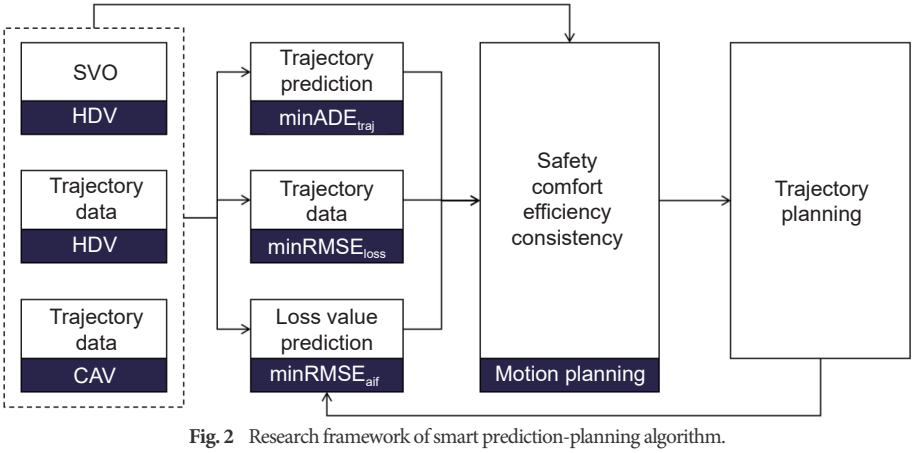

Fig. 2 Research framework of smart prediction-planning algorithm.

Table 1 Prediction models of F1 and F2

	F1	F2
Input	Trajectory data	Trajectory and SVO data
Training index	f_1	f_2
Output	Future trajectory	
Evaluation metrics	ADE, FDE, MR	

Note: The predicted trajectory of the HDV is $\boldsymbol{TP}_{\text{hdv,pred}} = [\boldsymbol{S}_{\text{hdv,pred}}(t+\Delta t), \boldsymbol{S}_{\text{hdv,pred}}(t+2\Delta t), \ldots, \boldsymbol{S}_{\text{hdv,pred}}(t+q\Delta t)]^T$, $q = \lfloor T/\Delta t \rfloor$, where T is the time domain (s), and Δt is the update frequency (s). The real trajectory of HDV is $\boldsymbol{TP}_{\text{hdv,true}} = [\boldsymbol{S}_{\text{hdv,true}}(t+\Delta t), \boldsymbol{S}_{\text{hdv,true}}(t+2\Delta t), \ldots, \boldsymbol{S}_{\text{hdv,true}}(t+q\Delta t)]^T$.

as CAVs in this study) and can automatically learn typical interactions between different vehicle trajectories. The output data are HDV future trajectory data $\boldsymbol{TP}_{\text{hdv,pred}}$. For the single-modal trajectory prediction model, ADE, FDE, and MR are selected as evaluation indicators (Table 1).

Input data for F1. Vehicle trajectory prediction has obvious time series characteristics. The input data of F1 include HDV trajectory data $\boldsymbol{TP}_{\text{hdv,history}}$ and CAV trajectory data $\boldsymbol{TP}_{\text{cav,history}}$.

Training index for F1. We calculate it by the vector angle between the HDV-predicted trajectory and the real trajectory and the L1 distance loss value.

$$f_1 = \frac{\alpha_1}{q}\sum_{i=1}^{q} L_{\text{lat}}\left[\boldsymbol{S}_{\text{hdv,pred}}\left(t+i\cdot\Delta t\right),\boldsymbol{S}_{\text{hdv,real}}\left(t+i\cdot\Delta t\right)\right] + \frac{\alpha_2}{q}\sum_{i=1}^{q} L_{\text{lon}}\left[\boldsymbol{S}_{\text{hdv,pred}}\left(t+i\cdot\Delta t\right),\boldsymbol{S}_{\text{hdv,real}}\left(t+i\cdot\Delta t\right)\right] \tag{1}$$

$$L_{\text{lat}}\left[\boldsymbol{S}_{\text{hdv,pred}}\left(t+i\cdot\Delta t\right),\boldsymbol{S}_{\text{hdv,real}}\left(t+i\cdot\Delta t\right)\right] = L_{\text{loss}}\left[\boldsymbol{S}_{\text{hdv,pred}}\left(t+i\cdot\Delta t\right),\boldsymbol{S}_{\text{hdv,real}}\left(t+i\cdot\Delta t\right)\right] \times \sin\left(\Delta\boldsymbol{S}^i_{\text{hdv,pred}},\Delta\boldsymbol{S}^i_{\text{hdv,real}}\right) \tag{2}$$

$$L_{\text{lon}}\left[\boldsymbol{S}_{\text{hdv,pred}}\left(t+i\cdot\Delta t\right),\boldsymbol{S}_{\text{hdv,real}}\left(t+i\cdot\Delta t\right)\right] = L_{\text{loss}}\left[\boldsymbol{S}_{\text{hdv,pred}}\left(t+i\cdot\Delta t\right),\boldsymbol{S}_{\text{hdv,real}}\left(t+i\cdot\Delta t\right)\right] \times \cos\left(\Delta\boldsymbol{S}^i_{\text{hdv,pred}},\Delta\boldsymbol{S}^i_{\text{hdv,real}}\right) \tag{3}$$

$$L_{\text{loss}}\left[\boldsymbol{S}_{\text{hdv,pred}}\left(t+i\cdot\Delta t\right),\boldsymbol{S}_{\text{hdv,real}}\left(t+i\cdot\Delta t\right)\right] = \sum_{i=1}^{q}\left|\boldsymbol{S}_{\text{hdv,pred}}\left(t+i\cdot\Delta t\right)-\boldsymbol{S}_{\text{hdv,real}}\left(t+i\cdot\Delta t\right)\right| \tag{4}$$

$$\sin\left(\Delta\boldsymbol{S}^i_{\text{hdv,pred}},\Delta\boldsymbol{S}^i_{\text{hdv,real}}\right) = \sqrt{1-\cos^2\left(\Delta\boldsymbol{S}^i_{\text{hdv,pred}},\Delta\boldsymbol{S}^i_{\text{hdv,real}}\right)} \tag{5}$$

$$\cos\left(\Delta\boldsymbol{S}^i_{\text{hdv,pred}},\Delta\boldsymbol{S}^i_{\text{hdv,real}}\right) = \frac{\Delta\boldsymbol{S}^i_{\text{hdv,pred}}\cdot\Delta\boldsymbol{S}^i_{\text{hdv,real}}}{\left|\Delta\boldsymbol{S}^i_{\text{hdv,pred}}\right|\cdot\left|\Delta\boldsymbol{S}^i_{\text{hdv,real}}\right|} \tag{6}$$

$$\Delta\boldsymbol{S}^i_{\text{hdv,pred}} = \boldsymbol{S}_{\text{hdv,pred}}\left(t+i\cdot\Delta t\right)-\boldsymbol{S}_{\text{hdv,pred}}\left[t+(i-1)\cdot\Delta t\right] \tag{7}$$

$$\Delta\boldsymbol{S}^i_{\text{hdv,real}} = \boldsymbol{S}_{\text{hdv,real}}\left(t+i\cdot\Delta t\right)-\boldsymbol{S}_{\text{hdv,real}}\left[t+(i-1)\cdot\Delta t\right] \tag{8}$$

where f_1 is the training indicator of the HDV trajectory prediction model during the training process. α_1 and α_2 are the weights for the lateral and longitudinal deviations, respectively. q is the number of trajectory points. $L_{\text{lat}}[\boldsymbol{S}_{\text{hdv,pred}}(t+i\cdot\Delta t), \boldsymbol{S}_{\text{hdv,real}}(t+i\cdot\Delta t)]$ is the lateral deviation for the predicted and real trajectories of the HDV at the i-th trajectory point. $L_{\text{lon}}[\boldsymbol{S}_{\text{hdv,pred}}(t+i\cdot\Delta t), \boldsymbol{S}_{\text{hdv,real}}(t+i\cdot\Delta t)]$ is the longitudinal deviation for the predicted and real trajectories of the HDV at the i-th trajectory point. $L_{\text{loss}}[\boldsymbol{S}_{\text{hdv,pred}}(t+i\cdot\Delta t), \boldsymbol{S}_{\text{hdv,real}}(t+i\cdot\Delta t)]$ is the total deviation for the predicted and real trajectories of the HDV at the i-th trajectory point. The $\sin(\Delta\boldsymbol{S}^i_{\text{hdv,pred}}, \Delta\boldsymbol{S}^i_{\text{hdv,real}})$ is the sine value between $\Delta\boldsymbol{S}^i_{\text{hdv, pred}}$ and $\Delta\boldsymbol{S}^i_{\text{hdv, real}}$. The $\cos(\Delta\boldsymbol{S}^i_{\text{hdv, pred}}, \Delta\boldsymbol{S}^i_{\text{hdv, real}})$ is the cosine between $\Delta\boldsymbol{S}^i_{\text{hdv, pred}}$ and $\Delta\boldsymbol{S}^i_{\text{hdv, real}}$. $\Delta\boldsymbol{S}^i_{\text{hdv, pred}}$ is the deviation between the i-th and $(i-1)$-th predicted trajectories. $\Delta\boldsymbol{S}^i_{\text{hdv, real}}$ is the deviation between the i-th and $(i-1)$-th predicted trajectories. The prediction model at this time is F1.

Driver factors are important reference indicators that affect the future trajectory selection of HDVs. Therefore, the difference from F1 is that F2 optimizes the input data and training indicators. The output data, prediction model, and evaluation metrics remain unchanged.

Input data for F2. The data input of F2 includes HDV trajectory data $\boldsymbol{TP}_{\text{hdv, history}}$, CAV trajectory data $\boldsymbol{TP}_{\text{cav, trajectory}}$, and D-SVO**.** The output data are HDV future trajectory data $\boldsymbol{TP}_{\text{hdv,pred}}$.

Training index for F2. On the basis of F1, the D-SVO distribution model of the HDV is introduced. When the HDV and CAV participate in game interaction, D-SVO can better evaluate its future trajectory choices. When the HDV and CAV gradually break away from the game interaction, D-SVO's performance in correcting trajectory prediction results decreases. The problem is that the real future trajectory of an HDV considers "driver characteristics" and the "surrounding road environment" at the same time, that is, the joint result of subjective factors and objective factors. Therefore, the training indicators $f_{\text{hdv,svo}}$ based on D-SVO are imported. All the indicators are normalized.

$$f_{\text{hdv,lat}} = \frac{1}{q}\sum_{i=1}^{q} L_{\text{lat}}\left[\boldsymbol{S}_{\text{hdv,pred}}\left(t+i\cdot\Delta t\right),\boldsymbol{S}_{\text{hdv,real}}\left(t+i\cdot\Delta t\right)\right] \tag{9}$$

$$f_{\text{hdv,lon}} = \frac{1}{q}\sum_{i=1}^{q} L_{\text{lon}}\left[\boldsymbol{S}_{\text{hdv,pred}}\left(t+i\cdot\Delta t\right),\boldsymbol{S}_{\text{hdv,real}}\left(t+i\cdot\Delta t\right)\right] \tag{10}$$

$$\begin{cases} f_{\text{hdv,svo}} = \dfrac{1}{q}\displaystyle\sum_{i=1}^{q}\beta_i\left|\text{D}-\text{SVO}^{\circ}_{\text{hdv,mean,pred}}\left(t+i\cdot\Delta t\right) - \text{D}-\text{SVO}^{\circ}_{\text{hdv,mean,real}}\left(t+i\cdot\Delta t\right)\right| \\ \beta_i = \dfrac{2}{1+e^{\text{D}-\text{SVO}^{\circ}_{\text{hdv,std}}\left(t+i\cdot\Delta t\right)}} \end{cases} \tag{11}$$

$$\begin{cases} f_2 = \alpha_{\text{lat}} f_{\text{hdv,lat}} + \alpha_{\text{lon}} f_{\text{hdv,lon}} + \alpha_{\text{svo}} f_{\text{hdv,svo}} \\ \alpha_{\text{lat}} + \alpha_{\text{lon}} + \alpha_{\text{svo}} = 1 \end{cases} \tag{12}$$

where $f_{\text{hdv,lat}}$ is the deviation between the laterally predicted and real trajectory data of the HDVs. $f_{\text{hdv,lon}}$ is the deviation between the longitudinal predicted and real trajectory data of HDVs. $f_{\text{hdv,svo}}$ is the deviation between the predicted and real SVO of HDV drivers. β_i is the weight for the SVO at the i-th trajectory point. α_{lat}, α_{lon}, and α_{svo} are the weights for $f_{\text{hdv,lat}}$, $f_{\text{hdv,lon}}$, and $f_{\text{hdv,svo}}$, respectively. The prediction model at this time is F2.

3.2 Loss value prediction via SVO

Under the same trajectory planning algorithm, the loss values of different candidate trajectories need to be evaluated. Therefore, we can use the prediction model to directly predict CAV safety and consistency loss values and use the prediction results for CAV trajectory optimization. The real safety and consistency loss values of the CAV candidate trajectories are set to $J_{\text{safety,real}}$ and $J_{\text{consistency,real}}$. The predicted safety and consistency loss values of the candidate trajectories are $J_{\text{safety,pred}}$ and $J_{\text{consistency,pred}}$, respectively The training model is LSTM (Table 2).

Input data for F3. CAV safety and consistency loss values have obvious time series characteristics. The input data for F3's loss

Table 2 Prediction models of F3 and F4

	F3	F4
Input	Trajectory data, loss value	Trajectory data, loss value, SVO data
Training index	f_3	f_4
Output	Future loss value	
Evaluation metrics	RMSE	

value prediction include CAV safety value data $\boldsymbol{J}_{\text{safety,history}} = [J_{\text{safety,real}}(t - t_0), J_{\text{safety,real}}(t - 2t_0), \ldots]$, CAV consistency loss value data $\boldsymbol{J}_{\text{consistency,history}} = [J_{\text{consistency,real}}(t - t_0), J_{\text{consistency,real}}(t - 2t_0), \ldots]$, HDV trajectory data $\boldsymbol{TP}_{\text{hdv,history}}$, and CAV trajectory data $\boldsymbol{TP}_{\text{cav,trajectory}}$. The output data are the future safety and consistency loss values $J_{\text{safety,pred}}$ and $J_{\text{consistency,pred}}$, respectively of CAV at each timestamp.

Training index for F3. We model f_3 through the predicted safety and consistency loss values of CAV and the true safety and consistency loss values.

$$f_3 = \left[\frac{K_{\text{safety}}}{q} \sum_{i=1}^{q} \left| J_{\text{safety,real}}(t + i \cdot \Delta t) - J_{\text{safety,pred}}(t + i \cdot \Delta t) \right| + \frac{K_{\text{consistency}}}{q} \sum_{i=1}^{q} \left| J_i(t + i \cdot \Delta t) - J_{\text{consistency,pred}}(t + i \cdot \Delta t) \right| \right] \tag{13}$$

Driver factors are important factors affecting CAV safety and consistency loss values. Therefore, F4 optimizes the input data and training indicators. The output data, prediction model, and evaluation metrics remain unchanged.

Input data for F4. The data input of F4 includes CAV safety value data $\boldsymbol{J}_{\text{safety,history}} = [J_{\text{safety,real}}(t - t_0), J_{\text{safety,real}}(t - 2t_0), \ldots]$, CAV consistency loss value data $\boldsymbol{J}_{\text{consistency,history}} = [J_{\text{consistency,real}}(t - t_0), J_{\text{consistency,real}}(t - 2t_0), \ldots]$, HDV trajectory data $TP_{\text{hdv,history}}$, CAV trajectory data $TP_{\text{cav,trajectory}}$, and HDV's D-SVO data. The output data are the future safety and consistency loss values $J_{\text{safety,pred}}$ and $J_{\text{consistency,pred}}$, respectively of CAV at each timestamp.

Training index for F4. When the HDV and CAV participate in game interaction, the HDV's D-SVO can better evaluate the choice of the CV's future trajectory. When the HDV and CAV gradually break away from the game interaction, the HDV's D-SVO performance in correcting trajectory prediction results decreases. Ideally, future trajectory prediction for HDVs is based on the historical trajectory of the HDV and the status data of the CAV. Without considering driver characteristics, F3's training indicators are reasonable. The problem is that the real future trajectory of an HDV considers "driver characteristics" and the "surrounding road environment" at the same time, that is, the joint result of subjective factors and objective factors. Therefore, the HDV prediction model must consider subjective factors to ensure that the prediction results approach the real situation. All the indicators are normalized.

$$f_{\text{cav,safety}} = \frac{1}{q} \sum_{i=1}^{q} \left| J_{\text{safety,real}}(t + i \cdot \Delta t) - J_{\text{safety,pred}}(t + i \cdot \Delta t) \right| \tag{14}$$

$$f_{\text{cav,consistency}} = \frac{1}{q} \sum_{i=1}^{q} \left| J_{\text{consistency,real}}(t + i \cdot \Delta t) - J_{\text{consistency,pred}}(t + i \cdot \Delta t) \right| \tag{15}$$

$$\begin{cases} f_{\text{hdv,svo}} = \dfrac{1}{q} \displaystyle\sum_{i=1}^{q} \beta_i \left| \text{D} - \text{SVO}^{\circ}_{\text{hdv,mean,pred}}(t + i \cdot \Delta t) - \text{D} - \text{SVO}^{\circ}_{\text{hdv,mean,real}}(t + i \cdot \Delta t) \right| \\ \beta_i = \dfrac{2}{1 + e^{\text{D} - \text{SVO}^{\circ}_{\text{cv,std}}(t + i \cdot \Delta t)}} \end{cases} \tag{16}$$

$$f_4 = \alpha_{\text{safety}} \cdot f_{\text{cav,safety}} + \alpha_{\text{consistency}} \cdot f_{\text{cav,consistency}} + \alpha_{\text{svo}} \cdot f_{\text{hdv,svo}} \tag{17}$$

where $f_{\text{cav,safety}}$ is the deviation between the predicted and real safety loss values at the i-th trajectory point. $f_{\text{cav,consistency}}$ is the deviation between the predicted and real consistency loss values at the i-th trajectory point. α_{safety}, $\alpha_{\text{consistency}}$, and α_{svo} are the weights for $f_{\text{cav,safety}}$, $f_{\text{cav,consistency}}$, and $f_{\text{hdv,svo}}$, respectively. The prediction model at this time is F4.

3.3 Loss value prediction via smart predict-planning

With the advancement of autonomous vehicle technology, both the prediction and planning modules have achieved strong performance in their respective functions. However, the challenge of information loss between these modules remains a critical issue, especially in complex corner cases. To address this, a new training metric that incorporates the objectives of the planning module into the prediction module is proposed (Mo and Lv, 2023). This metric aims to minimize the information loss between distinct modules, thereby enhancing the integration of the prediction and planning processes in CAVs (Chen et al., 2023).

The HDVs that interact with CAVs are the I_{HDV} vehicles. The safety loss value generated by HDV$_i$ at the j-th candidate trajectory of a CAV is $J_{\text{safety}(i,j)}$, the consistency loss value is $J_{\text{consistency}(i,j)}$ ($I = 1, 2, \ldots, I_{\text{HDV}}$), and for the j-th CAV, the objective functions of the candidate trajectories include the safety function $J_{\text{safety}(j)}$, the comfort function $J_{\text{comfort}(j)}$, the efficiency function $J_{\text{efficiency}(j)}$, and the consistency function $J_{\text{consistency}(j)}$. The expressions of the safety and consistency functions are as

$$J_{\text{safety}(j)} = \sum_{i=1} \alpha_{(i)} \cdot J_{\text{safety}(i,j)} \tag{18}$$

$$J_{\text{consistency}(j)} = \sum_{i=1} \beta_{(i)} \cdot J_{\text{consistency}(i,j)} \tag{19}$$

where $\alpha_{(i)}$ represents the safety weight of the HDV$_i$ relative to the CAV candidate trajectories and where $\beta_{(i)}$ represents the consistency weight of the HDV$_i$ relative to the CAV candidate trajectories.

This study uses the traditional potential energy field and D-SVO to define two weight distributions. The potential energy field strength generated by HDV$_i$ at the CAV is set as $\boldsymbol{E}_i$, the D-SVO of the HDV$_i$ driver is set as D-SVO$_i$, and the corresponding angle is set as D-SVO_i°. Psychological research has shown that SVO is a key factor that affects individual behavior and attitudes in a wide range of social situations. Compared with self-centered people, prosocial people exhibit more trust and cooperation behaviors, and prosocial people act on behalf of others. Performance in decision-making is more similar to decision-making for oneself; that is, prosocials' self-other decision-making discrepancies are smaller. The first is the safety weight $\alpha_{(i)}$. From the analysis of explicit factors, $\boldsymbol{E}_i$ is taken as the basic element. The larger the value is, the greater the safety weight $\alpha_{(i)}$ of HDV$_i$. From the perspective of implicit factors, when different HDV$_i$ values have the same $|\boldsymbol{E}_i|$ (the directions may differ), proself drivers may make more radical and self-interested driving decisions than prosocial drivers. The second is the consistency weight $\beta_{(i)}$. As mentioned above, prosocial drivers have smaller self-other decision-making differences than proself drivers do, so the consistency weight $\beta_{(i)}$ of prosocial drivers is greater. Therefore, we can use HDV$_i$'s $\boldsymbol{E}_i$ and D-SVO_i° to define $\alpha_{(i)}$ and use D-SVO_i° to define $\beta_{(i)}$. The expressions of $\alpha_{(i)}$ and $\beta_{(i)}$ are as

$$\alpha_i = \frac{\sigma\left(\text{D-SVO}_i^{\circ\prime}\right) \cdot e^{|\boldsymbol{E}_i|}}{\sum_{i=1} \sigma\left(\text{D-SVO}_i^{\circ\prime}\right) \cdot e^{|\boldsymbol{E}_i|}}, \quad \beta_i = \frac{e^{\text{D-SVO}_i^{\circ\prime}}}{\sum_{i=1} e^{\text{D-SVO}_i^{\circ\prime}}} \tag{20}$$

$$\sigma\left(\text{D-SVO}_i^{\circ\prime}\right)=\frac{1}{1+\mathrm{e}^{-\text{D-SVO}_i^{\circ\prime}}} \tag{21}$$

$$\text{D-SVO}_i^{\circ\prime}=\frac{\text{D-SVO}_i^{\circ}-\text{D-SVO}_{i-\min}^{\circ}}{\text{D-SVO}_{i-\max}^{\circ}-\text{D-SVO}_{i-\min}^{\circ}} \tag{22}$$

$$|\boldsymbol{E}_i'|=\frac{|\boldsymbol{E}_i|-|\boldsymbol{E}_{\min}|}{|\boldsymbol{E}_{\max}|-|\boldsymbol{E}_{\min}|} \tag{23}$$

Therefore, the CAV only needs to screen out the trajectories corresponding to the lowest value of the total loss value C_{total} among all its candidate trajectories. The optimization goal of CAV is to find the relative minimum value of the total loss value.

We analyze the relationships among different data in four stages and derive training indicators for the prediction model.

Step 1: The CAV has generated n candidate trajectories, and the total loss value of each candidate trajectory is $\boldsymbol{C}_{\text{total}}=[C_{\text{total}(1)}, C_{\text{total}(2)}, \ldots, C_{\text{total}(n)}]$. The weight values of the CAV safety, comfort, efficiency, and consistency functions are K_{safety}, K_{comfort}, $K_{\text{efficiency}}$, and $K_{\text{consistency}}$, respectively. The solution matrix for all candidate trajectories is as

$$\begin{bmatrix} C_{\text{total}(1)} \\ C_{\text{total}(2)} \\ \cdots \\ C_{\text{total}(n)} \end{bmatrix} = \begin{bmatrix} J_{\text{safety}(1)} & J_{\text{comfort}(1)} & J_{\text{efficiency}(1)} & J_{\text{consistency}(1)} \\ J_{\text{safety}(2)} & J_{\text{comfort}(2)} & J_{\text{efficiency}(2)} & J_{\text{consistency}(2)} \\ \cdots & \cdots & \cdots & \cdots \\ J_{\text{safety}(n)} & J_{\text{comfort}(n)} & J_{\text{efficiency}(n)} & J_{\text{consistency}(n)} \end{bmatrix} \times \begin{bmatrix} K_{\text{safety}} \\ K_{\text{comfort}} \\ K_{\text{efficiency}} \\ K_{\text{consistency}} \end{bmatrix} \tag{24}$$

where the predicted total loss value of the j-th candidate trajectory of the CAV is $C_{\text{total-pred}(j)}$ and the true total loss value is $C_{\text{total-true}(j)}$. The predicted safety loss value of the j-th candidate trajectory is $J_{\text{safety-pred}(j)}$ (HDV$_i$'s predicted safety loss value is $J_{\text{safety-pred}(i,j)}$), and the true safety loss value is $J_{\text{safety-true}(j)}$ (HDV$_i$'s true safety loss value is $J_{\text{safety-true}(i,j)}$). The predicted consistency loss value is $J_{\text{consistency-pred}(j)}$ (the predicted consistency loss value of HDV$_i$ is $J_{\text{consistency-pred}(i,j)}$), and the true consistency loss value is $J_{\text{consistency-true}(j)}$ (the true consistency loss value of HDV$_i$ is $J_{\text{consistency-true}(i,j)}$).

Step 2: Derive the relationship between the predicted results and the real results.

$$J_{\text{safety-true}(i,j)}-J_{\text{safety}-\text{pred}(i,j)}=\Delta J_{\text{safety}(i,j)} \tag{25}$$

$$J_{\text{consistency-true}(i,j)}-J_{\text{consistency-pred}(i,j)}=\Delta J_{\text{consistency}(i,j)} \tag{26}$$

$$C_{\text{total-true}(j)}-C_{\text{total-pred}(j)}=\Delta C_{\text{total}(j)} \tag{27}$$

Expanding Eqs. (24)–(26), we obtain the following results:

$$K_{\text{safety}}\cdot\left[J_{\text{safety-trus}(j)}-J_{\text{safety-pred}(j)}\right]+K_{\text{consistency}}\cdot\left[J_{\text{consistency-true}(j)}-J_{\text{consistency-pred}(j)}\right]=\Delta C_{\text{total}(j)} \tag{28}$$

$J_{\text{safety-trus}(j)}=\sum_{i=1}\alpha_i\cdot J_{\text{safety-trus}(i,j)}$, $J_{\text{safety-pred}(j)}=\sum_{i=1}\alpha_i\cdot J_{\text{safety-pred}(i,j)}$, $J_{\text{consistency-true}(j)}=\sum_{i=1}\beta_i\cdot J_{\text{consistency-true}(i,j)}$, $J_{\text{consistency-pred}(j)}=\sum_{i=1}\beta_i\cdot J_{\text{consistency-pred}(i,j)}$, and Eq. (27) becomes Eq. (28) as

$$K_{\text{safety}}\cdot\sum_{i=1}\alpha_i\cdot\left(J_{\text{safety-trus}(i,j)}-J_{\text{safety-pred}(i,j)}\right)+K_{\text{consistency}}\times\sum_{i=1}\beta_i\cdot\left(J_{\text{consistency-true}(i,j)}-J_{\text{consistency-pred}(i,j)}\right)=\Delta C_{\text{total}(j)} \tag{29}$$

Equations (28) and (29) are combined into Eq. (30) as

$$K_{\text{safety}}\cdot\sum_{i=1}\alpha_i\cdot\Delta J_{\text{safety}(i,j)}+K_{\text{consistency}}\cdot\sum_{i=1}\beta_i\cdot\Delta J_{\text{consistency}(i,j)}=\Delta C_{\text{total}(j)} \tag{30}$$

Step 3: Case analysis. Theoretically, we need to compare the size relationship between the total loss values of all candidate trajectories of CAVs. For example, CAV has three candidate trajectories, 1, 2, and 3, and the corresponding total loss values are $C_{\text{total-true}(1)}/C_{\text{total-pred}(1)}$, $C_{\text{total-true}(2)}/C_{\text{total-pred}(2)}$, and $C_{\text{total-true}(3)}/C_{\text{total-pred}(3)}$.

$$C_{\text{total-trus}(1)}-C_{\text{total-trus}(2)}=C_{\text{true}(1\to2)} \tag{31}$$

$$C_{\text{total-trus}(2)}-C_{\text{total-trus}(3)}=C_{\text{true}(2\to3)} \tag{32}$$

$$C_{\text{total-pred}(1)}-C_{\text{total-pred}(2)}=C_{\text{pred}(1\to2)} \tag{33}$$

$$C_{\text{total-pred}(2)}-C_{\text{total-pred}(3)}=C_{\text{pred}(2\to3)} \tag{34}$$

$$C_{\text{total-trus}(1)}-C_{\text{total-pred}(1)}=\Delta C_{\text{total}(1)} \tag{35}$$

$$C_{\text{total-trus}(2)}-C_{\text{total-pred}(2)}=\Delta C_{\text{total}(2)} \tag{36}$$

$$C_{\text{total-trus}(3)}-C_{\text{total-pred}(3)}=\Delta C_{\text{total}(3)} \tag{37}$$

Comparing Eq. (35) to Eq. (36) and Eq. (36) to Eq. (37), the following results are obtained:

$$C_{\text{true}(1\to2)}-C_{\text{pred}(1\to2)}=\Delta C_{\text{total}(1)}-\Delta C_{\text{total}(2)} \tag{38}$$

$$C_{\text{true}(2\to3)}-C_{\text{pred}(2\to3)}=\Delta C_{\text{total}(2)}-\Delta C_{\text{total}(3)} \tag{39}$$

Substitute Eq. (30) into Eq. (38) and Eq. (39).

$$C_{\text{true}(1\to2)}=K_{\text{safety}}\cdot\sum_{i=1}\alpha_i\cdot\left[\Delta J_{\text{safety}(i,1)}-\Delta J_{\text{safety}(i,2)}\right]+K_{\text{consistency}}\times\sum_{i=1}\beta_i\cdot\left[\Delta J_{\text{consistency}(i,1)}-\Delta J_{\text{consistency}(i,2)}\right]+C_{\text{pred}(1\to2)} \tag{40}$$

$$C_{\text{true}(2\to3)}=K_{\text{safety}}\cdot\sum_{i=1}\alpha_i\cdot\left[\Delta J_{\text{safety}(i,2)}-\Delta J_{\text{safety}(i,3)}\right]+K_{\text{consistency}}\times\sum_{i=1}\beta_i\cdot\left[\Delta J_{\text{consistency}(i,2)}-\Delta J_{\text{consistency}(i,3)}\right]+C_{\text{pred}(2\to3)} \tag{41}$$

Therefore, according to the case situation, when the safety loss value and consistency loss value of CAVs for HDV$_i$ with different driving conditions and different SVOs satisfy the above equations, the prediction results of safety and consistency loss values do not affect the actual optimization result.

Step 4: Transition from the case scenario to the regular scenario. Assume that a CAV has n candidate trajectories. The

relative relationship between the j_1 trajectory and the j_2 trajectory $(j_1 < j_2)$ is as

$$C_{\text{true}(j_1 \to j_2)} = K_{\text{safety}} \cdot \sum_{i=1} \alpha_i \cdot [\Delta J_{\text{safety}(i,j_1)} - \Delta J_{\text{safety}(i,j_2)}] + K_{\text{consistency}} \cdot \sum_{i=1} \beta_i \cdot [\Delta J_{\text{consistency}(i,j_1)} - \Delta J_{\text{consistency}(i,j_2)}] + C_{\text{pred}(j_1 \to j_2)} \tag{42}$$

There are a total of $(n^2 - n) / 2$ cases when traversing $j_1 < j_2$, as long as $g(j_1, j_2) > 0$ is satisfied.

$$g(j_1, j_2) = C_{\text{true}(j_1 \to j_2)} \cdot \left\{ K_{\text{safety}} \cdot \sum_{i=1} \alpha_i \cdot [\Delta J_{\text{safety}(i,j_1)} - \Delta J_{\text{safety}(i,j_2)}] + K_{\text{consistency}} \cdot \sum_{i=1} \beta_i \cdot [\Delta J_{\text{consistency}(i,j_1)} - \Delta J_{\text{consistency}(i,j_2)}] + C_{\text{pred}(j_1 \to j_2)} \right\} \tag{43}$$

When $g(j_1, j_2) > 0$, the prediction result has a better effect on the optimization result, and the output result is recorded as 0. Conversely, when $g(j_1, j_2) \le 0$, the prediction result has a worse effect on the optimization result.

Therefore, we obtain training indicators guided by planning objectives, as shown in Eq. (44):

$$f = \sum_{j_2 > j_1}^{n} \sum_{j_1 = 1}^{n} G(j_1, j_2)$$
$$G(j_1, j_2) = \begin{cases} 0, & g(j_1, j_2) > 0 \\ \dfrac{1}{1 + e^{-|g(j_1, j_2)|}}, & g(j_1, j_2) \leqslant 0 \end{cases} \tag{44}$$

where $G(j_1, j_2)$ represents the training metrics for the j_1 trajectory and j_2 trajectory.

The prediction model at this time is F5.

4 Motion planning model

For CAVs, we introduce SVO-driven motion planning. The planning model calculates the total cost of each candidate trajectory by incorporating the SVO-influenced behaviors of surrounding vehicles. This involves adjusting the weights assigned to safety, comfort, efficiency and consistency in the cost function. A vehicle with a cooperative SVO might prioritize safety over efficiency, whereas a self-focused vehicle prioritizes minimizing travel time. In the planning model, SVO plays a key role in shaping the motion planning process of CAVs, as it selects the optimal future trajectory. This approach is grounded in utility-based motion planning and risk-aware models.

Utility-based motion planning. In the planning model, the vehicle evaluates multiple candidate trajectories and selects the one that maximizes a utility function, which incorporates SVO-based considerations. This utility function not only focuses on self-oriented objectives, such as minimizing travel time or maximizing comfort but also accounts for the broader social environment by prioritizing safety, cooperation, and compliance with traffic rules. Utility maximization is a central concept in decision theory, where rational agents aim to maximize their utility under given constraints. SVO modifies the utility function by introducing weights for cooperative versus self-interested behavior. A vehicle with a cooperative SVO assigns higher utility to trajectories that maintain safe distances or yield to others, whereas a self-interested vehicle seeks to maximize its own efficiency. This approach parallels the social utility models in behavioral economics, where agents consider both individual and collective payoffs when making decisions in social contexts.

Risk-aware models. Another theoretical foundation for SVO in planning is its alignment with risk-aware decision models. Driving is inherently risky, requiring trade-offs between safety, comfort, and efficiency. SVO aids the planning model in assessing risk not only from the perspective of the autonomous vehicle but also from the broader traffic environment, where the actions of other vehicles can introduce additional risks. A vehicle with a cooperative SVO may plan a more conservative trajectory, maintaining larger distances from other vehicles to reduce the likelihood of collisions. In contrast, a more self-interested vehicle might take greater risks to optimize for time efficiency. By adjusting the risk profile of each trajectory via SVO, the planning model can balance these trade-offs in a manner that mirrors real-world driving behavior. This approach is grounded in bounded rationality and prospect theory, which explain how agents make decisions under uncertainty by factoring in both potential gains and risks. SVO enriches this framework by introducing a social layer to risk assessment, allowing vehicles to plan trajectories that reflect both personal and social risk considerations.

4.1 Parameter description of CAV

In the global coordinate system, the state data of the CAV at time t are $\boldsymbol{S}_{\text{cav}} = [x_{\text{cav}}, y_{\text{cav}}, v_{\text{cav}}, a_{\text{cav}}, \theta_{\text{cav}}, \kappa_{\text{cav}}]^T$, where x_{cav} represents lateral position, y_{cav} represents longitudinal position, v_{cav} represents speed, a_{cav} represents acceleration, θ_{cav} represents deflection angle, and κ_{cav} represents curvature. The status data of the HDV are $\boldsymbol{S}_{\text{hdv}} = [x_{\text{hdv}}, y_{\text{hdv}}, v_{\text{hdv}}, a_{\text{hdv}}, \theta_{\text{hdv}}, \kappa_{\text{hdv}}]^T$, and the future trajectory data of the HDV are $\boldsymbol{TP}_{\text{hdv}} = [S_{\text{hdv}}(t), S_{\text{hdv}}(t + \Delta t), S_{\text{hdv}}(t + 2\Delta t), \ldots, S_{\text{hdv}}(t + q\Delta t)]^T$, where $q = \lfloor T/\Delta t \rfloor$, T is the trajectory planning time domain (s), and Δt is the trajectory update frequency (s). The decision result of the CAV is $DM_{\text{cav}} = f_{\text{cav}}([DP_{\text{cav}}, DS_{\text{cav}}, DG_{\text{cav}}]^T)$.

Existing trajectory planning algorithms are mainly based on graph algorithms, optimization algorithms, sampling algorithms or hybrid algorithms to meet the computing needs of different specific traffic scenarios. The problem is that CAVs and HDVs will coexist for a long time in the future, so trajectory planning algorithms that consider driver characteristics are very important. On the basis of the D-SVO algorithm constructed in previous studies, this study constructs an autonomous driving trajectory planning algorithm that fully considers D-SVO. The basic algorithm of trajectory planning adopts a hybrid algorithm, horizontal trajectory planning utilizes a sampling algorithm, and the longitudinal trajectory planning sampling optimization algorithm is obtained. CAV high-performance candidate trajectories.

4.2 Improved objective function considering consistency

First, the CAV fits and generates multiple high-quality candidate trajectories on the basis of the horizontal sampling algorithm and the vertical optimization algorithm. Second, this section constructs a dynamic objective optimization function by introducing driving consistency $J_{\text{consistency}}$ in addition to safety J_{safety}, comfort J_{comfort}, and efficiency $J_{\text{efficiency}}$ in the objective function.

4.2.1 Safety function

First, the safety loss value is calculated between the states of the CAV and the interacting HDV. When we obtain the future

trajectory of the HDV from the prediction module and the candidate trajectories of the CAV, the safety potential field strength value can be calculated at each trajectory point at the same timestamp. Finally, the safety loss value is generated by the average safety potential field strength value from the first point to the end point. For CAVs to navigate safely, they must consider both their current risk profile and that of surrounding HDVs concurrently. This comprehensive assessment forms the basis for quantitatively evaluating the relative safety of multiple CAV candidate trajectories with the predicted HDV trajectories. The safety function, denoted as J_{safety}, comprises two key components: an evaluation based on the instantaneous states of the CAV and HDV and another based on the predicted trajectories of CAV candidates and HDVs. The security weight values w_{present} and w_{future} assign importance to the state-based and trajectory-based safety assessments, respectively, with their sum equaling unity ($w_{\text{present}} + w_{\text{future}} = 1$). $\boldsymbol{E}_{\text{hdv}\to\text{cav}}$ represents the field strength generated by the HDV on the CAV, and $\boldsymbol{E}_{\max}$ denotes the maximum possible field strength. Moreover, within the trajectory-based evaluation, each trajectory point in the time series is assigned a weight, w_i, which exhibits an exponential decay trend; meaning that the impact of points further back in time diminishes. The sum of all weights, w_i, equals 1, ensuring a balanced consideration of the entire trajectory.

$$J_{\text{safety}} = w_{\text{present}} \left| \frac{\boldsymbol{E}_{\text{hdv}\to\text{cav}}(t)}{\boldsymbol{E}_{\max}} \right| + w_{\text{future}} \frac{1}{q} \sum_{i=1}^{q} w_i \left| \frac{\boldsymbol{E}_{\text{hdv}\to\text{cav}}(t+q\Delta t)}{\boldsymbol{E}_{\max}} \right|, \quad \sum_{i=1}^{q} w_i = 1 \tag{45}$$

Additionally, the explanation of the safety potential field strength is expressed as

$$\boldsymbol{E}_{\text{hdv}\to\text{cav}} = \frac{GR_{\text{hdv}}M_{\text{hdv}}}{|R_{\text{hdv}\to\text{cav}}|^{k_1}} \frac{\boldsymbol{r}_{\text{hdv}\to\text{cav}}}{|r_{\text{hdv}\to\text{cav}}|} \exp\left(k_2 v_{\text{hdv}} \cos(\theta_{\text{hdv}})\right) \tag{46}$$

where $\boldsymbol{E}_{\text{hdv}\to\text{cav}}$ is the safety potential field strength value of CAVs based on the impact of HDVs. $\boldsymbol{r}_{\text{hdv}\to\text{cav}}$ is the distance between the CAV and HDV. k_1, k_2, and G are the undetermined coefficients. M_{hdv} is the equivalent mass of the HDV. R_{hdv} is the index of road conditions. v_{hdv} is the speed of the HDV. θ_{hdv} is the angle between the speed direction and $\boldsymbol{r}_{\text{hdv-cav}}$.

4.2.2 Comfort function

To determine the comfort metric, J_{comfort}, we employ first-order, second-order, and third-order partial derivatives of the lateral displacement of the CAV within the Frenet coordinate system with respect to its longitudinal displacement. These derivatives serve as indicators that quantify various aspects of the vehicle's lateral motion, contributing to the overall comfort evaluation. The weight values, w_{first}, w_{second}, and w_{third}, are assigned to each of these indicators, reflecting their relative importance in the overall comfort assessment. The sum of these weights is normalized to 1, ensuring a balanced consideration of all three derivatives in the calculation of J_{comfort}.

$$J_{\text{comfort}} = w_{\text{first}} \int l'(s)^2 \mathrm{d}s + w_{\text{second}} \int l''(s)^2 \mathrm{d}s + w_{\text{third}} \int l'''(s)^2 \mathrm{d}s \tag{47}$$

4.2.3 Efficiency function

The conventional approach to defining the efficiency function relies solely on the deviation between the CAV's speed and a predetermined target speed. However, this study innovates by introducing dynamic spatiotemporal occupancy metrics, U_s and U_b to formulate the efficiency function, $J_{\text{efficiency}}$. This approach offers a more nuanced and rational assessment of CAVs' future trajectory performance in terms of optimizing road usage and spatiotemporal efficiency. By considering the dynamic nature of traffic flow and the vehicle's interactions with its surroundings, this method provides a more comprehensive evaluation framework that goes beyond traditional speed-based metrics.

$$J_{\text{efficiency}} = \frac{1}{q} \left[\sum_{i=1}^{q} U_s(t+q\Delta t) + \sum_{i=1}^{q} U_t(t+q\Delta t) \right] \tag{48}$$

4.2.4 Consistency function

In the pursuit of maximizing driving efficiency through CAV trajectory planning, it is crucial to acknowledge the potential risk of driving instability arising from significant disparities between the future trajectory choices of HDVs and CAVs. To mitigate this concern, driving consistency emerges as a pivotal indicator that must be factored into the planning process. When CAV candidate trajectories align closely with the predicted trajectories of HDVs in terms of their performance characteristics, fluctuations that could lead to accidents or traffic congestion can be prevented. To quantify driving consistency, we introduce $J_{\text{consistency}}$, which is computed by analyzing the vector angles and L1 distance loss values between the predicted HDV trajectory and each CAV candidate trajectory. This analysis begins by determining the vector angles between the corresponding trajectory segments of the HDV prediction and each CAV candidate, encompassing both transverse and longitudinal vector angles in the global coordinate system. By doing so, we can assess the similarity in directional changes and the degree of alignment between the two trajectories, thereby providing a robust measure of driving consistency.

$$\cos\left(\Delta \boldsymbol{S}_{\text{cav}}^{j}, \Delta \boldsymbol{S}_{\text{hdv}}^{j}\right) = \frac{\Delta \boldsymbol{S}_{\text{cav}}^{j} \cdot \Delta \boldsymbol{S}_{\text{hdv}}^{j}}{\left|\Delta \boldsymbol{S}_{\text{cav}}^{j}\right| \cdot \left|\Delta \boldsymbol{S}_{\text{hdv}}^{j}\right|} \tag{49}$$

$$\sin\left(\Delta \boldsymbol{S}_{\text{cav}}^{j}, \Delta \boldsymbol{S}_{\text{hdv}}^{j}\right) = \sqrt{1 - \cos^2\left(\Delta \boldsymbol{S}_{\text{cav}}^{j}, \Delta \boldsymbol{S}_{\text{hdv}}^{j}\right)} \tag{50}$$

$$\Delta \boldsymbol{S}_{\text{cav}}^{j} = \boldsymbol{S}_{\text{cav}}(t + j \cdot \Delta t) - \boldsymbol{S}_{\text{cav}}[t + (j-1) \cdot \Delta t] \tag{51}$$

$$\Delta \boldsymbol{S}_{\text{hdv}}^{j} = \boldsymbol{S}_{\text{hdv}}(t + j \cdot \Delta t) - \boldsymbol{S}_{\text{hdv}}[t + (j-1) \cdot \Delta t] \tag{52}$$

where $\sin\left(\Delta \boldsymbol{S}_{\text{cav}}^{j}, \Delta \boldsymbol{S}_{\text{hdv}}^{j}\right)$ is the angle between transverse vectors and $\cos\left(\Delta \boldsymbol{S}_{\text{cav}}^{j}, \Delta \boldsymbol{S}_{\text{hdv}}^{j}\right)$ is the angle between longitudinal vectors.

Second, the L1 distance loss between the HDV-predicted trajectory segments and CAV candidate trajectory segments is calculated.

$$L_{\text{loss}}\left[\boldsymbol{S}_{\text{cav}}(t + j \cdot \Delta t), \boldsymbol{S}_{\text{hdv}}(t + j \cdot \Delta t)\right] = \frac{1}{q} \sum_{j=1}^{q} \left|\boldsymbol{S}_{\text{cav}}(t + j \cdot \Delta t), \boldsymbol{S}_{\text{hdv}}(t + j \cdot \Delta t)\right| \tag{53}$$

where L_{loss} is the L1 distance loss, $\boldsymbol{S}_{\text{cav}}(t + j{\cdot}\Delta t)$ is the j-th trajectory point of the CAV, and $\boldsymbol{S}_{\text{hdv}}(t{+}j{\cdot}\Delta t)$ is the j-th predicted trajectory point of the HDV.

The lateral and longitudinal distance losses of the prediction model are subsequently calculated on the basis of the vector angle and L1 distance loss.

$$L_{\text{lat}}\left[\boldsymbol{S}_{\text{cav}}\left(t+j\cdot\Delta t\right),\boldsymbol{S}_{\text{hdv}}\left(t+j\cdot\Delta t\right)\right]=L_{\text{loss}}\left[\boldsymbol{S}_{\text{cav}}\left(t+j\cdot\Delta t\right),\boldsymbol{S}_{\text{hdv}}\left(t+j\cdot\Delta t\right)\right]\times\sin\left(\Delta\boldsymbol{S}_{\text{cav}}^{j},\Delta\boldsymbol{S}_{\text{hdv}}^{j}\right)\tag{54}$$

$$L_{\text{lon}}\left[\boldsymbol{S}_{\text{cav}}\left(t+j\cdot\Delta t\right),\boldsymbol{S}_{\text{hdv}}\left(t+j\cdot\Delta t\right)\right]=L_{\text{loss}}\left[\boldsymbol{S}_{\text{cav}}\left(t+j\cdot\Delta t\right),\boldsymbol{S}_{\text{hdv}}\left(t+j\cdot\Delta t\right)\right]\times\cos\left(\Delta\boldsymbol{S}_{\text{cav}}^{j},\Delta\boldsymbol{S}_{\text{hdv}}^{j}\right)\tag{55}$$

where L_{lat} is the transverse distance loss and L_{lon} is the longitudinal distance loss.

L_{lat} and L_{lon} are used to construct the consistency index in this step.

$$J_{\text{consistency}}=\alpha_1\sum_{j=1}^{q}L_{\text{lat}}\left[\boldsymbol{S}_{\text{cav}}\left(t+j\cdot\Delta t\right),\boldsymbol{S}_{\text{hdv}}\left(t+j\cdot\Delta t\right)\right]+\alpha_2\sum_{j=1}^{q}L_i\left[\boldsymbol{S}_{\text{cav}}\left(t+j\cdot\Delta t\right),\boldsymbol{S}_{\text{hdv}}\left(t+j\cdot\Delta t\right)\right]\tag{56}$$

where α_1 and α_2 represent the weights of horizontal distance loss and longitudinal distance loss, respectively, and $\alpha_1+\alpha_2=1$.

D-SVO was then introduced to optimize $J_{\text{consistency}}$. The larger D-SVO° is, the larger the value of $J_{\text{consistency}}$. If $|\boldsymbol{E}_{\text{hdv}\to\text{cav}}|$ is smaller, the value of $J_{\text{consistency}}$ will be smaller.

$$J_{\text{consistency}}\leftarrow\left|\frac{\text{D-SVO}^{\circ}}{\text{SVO}_{\text{max}}^{\circ}}\right|\cdot\left|\frac{\boldsymbol{E}_{\text{hdv}\to\text{cav}}}{\boldsymbol{E}_{\text{max}}}\right|\cdot J_{\text{consistency}}\tag{57}$$

Second, J_{safety}, J_{comfort}, $J_{\text{efficiency}}$, and $J_{\text{consistency}}$ of all candidate trajectories of CAVs are normalized to obtain the normalized $\boldsymbol{J}'_{\text{safety}}$, $\boldsymbol{J}'_{\text{comfort}}$, $\boldsymbol{J}'_{\text{efficiency}}$, and $\boldsymbol{J}'_{\text{consistency}}$.

The expression of the comprehensive objective function is as follows. K_{safety}, K_{smooth}, $K_{\text{efficiency}}$, and $K_{\text{consistency}}$ represent the weight values of safety, comfort, efficiency, and consistency, respectively.

$$\begin{cases}C_{\text{total}}=K_{\text{safety}}\cdot J'_{\text{safety}}+K_{\text{comfort}}\cdot J'_{\text{comfort}}+K_{\text{efficiency}}\cdot J'_{\text{efficiency}}\\\qquad\quad+K_{\text{consistency}}\cdot J'_{\text{consistency}}\\K_{\text{safety}}+K_{\text{smooth}}+K_{\text{efficiency}}+K_{\text{consistency}}=1\end{cases}\tag{58}$$

The model at this time is M1.

4.2.5 *Optimization of the weight distribution*

D-SVO can be used to characterize the cooperation tendency of HDV drivers dynamically. See the Appendix for details of the modeling process. There is a certain degree of uncertainty in trajectory prediction itself, so the interaction between CAVs and HDVs needs to consider the impact of HDV driver characteristics. For example, C_{safety} is calculated under the same HDV predicted trajectory and CAV candidate trajectory. Theoretically, the driving risk of a proself-type driver will be significantly greater than that of a prosocial driver, resulting in a CAV's failure to evaluate the relative risk of the two. The impact is also different. Therefore, we can improve the algorithm's adaptability to different HDVs by dynamically optimizing K_{safety}, K_{smooth}, $K_{\text{efficiency}}$, and $K_{\text{consistency}}$. The mean value of HDV's D-SVO is $\text{D-SVO}_{\text{hdv,mean}}^{\circ}$, and the standard deviation of D-SVO is $\text{D-SVO}_{\text{hdv,std}}^{\circ}$. When CAVs and HDVs choose different decision-making behaviors, there are differences in the CAV objective function. Vehicle decision-making content includes decision-making to pass, decision-making to slow down, and decision-making to yield. The situation where both vehicles decide to pass is not considered for the time being. For different CAV-HDV decision combination results, the corresponding initialization weights are proposed as $K_{\text{safety-0}}$, $K_{\text{smooth-0}}$, $K_{\text{efficiency-0}}$, and $K_{\text{consistency-0}}$. On this basis, if the mean value of $\text{D-SVO}_{\text{hdv,mean}}^{\circ}$ is larger, HDV prosocial behavior will be more obvious, and proself-type behavior will be more obvious. Therefore, the coefficient δ is introduced to evaluate the impact of $\text{D-SVO}_{\text{hdv,mean}}^{\circ}$ on the CAV objective function.

$$\delta=\text{e}^{q_1\left(\left|\frac{\text{S-SVO}_{\text{hdv}}^{\circ}}{\text{D-SVO}_{\text{hdv,mean}}^{\circ}}\right|-1\right)}-1\tag{59}$$

Moreover, when the standard deviation is too large, the uncertainty of the D-SVO distribution of the HDV is large at this time, and the interaction between the CAV and HDV is not obvious. At this time, the δ of CAV is infinitely far from the mean of D-SVO. When the standard deviation decreases, the D-SVO distribution of the HDV is relatively clear at this time, and the interactive game between the CAV and HDV is obvious. At this time, the δ of CAV is infinitely close to the mean of D-SVO.

$$\delta_{\text{update}}=\left(\frac{2}{1+e^{-q_2\text{D-SVO}_{\text{hdv,std}}^{\circ}}}\right)\delta\tag{60}$$

On this basis, the weights are further corrected as

$$K_{\text{safety}}\leftarrow\frac{\delta_{\text{update}}\cdot K_{\text{safety}}}{(\delta_{\text{update}}-1)\cdot K_{\text{safety}}+1}\tag{61}$$

$$K_{\text{comfort}}\leftarrow\frac{K_{\text{comfort}}}{(\delta_{\text{update}}-1)\cdot K_{\text{safety}}+1}\tag{62}$$

$$K_{\text{efficiency}}\leftarrow\frac{K_{\text{efficiency}}}{(\delta_{\text{update}}-1)\cdot K_{\text{safety}}+1}\tag{63}$$

$$K_{\text{consistency}}\leftarrow\frac{K_{\text{consistency}}}{(\delta_{\text{update}}-1)\cdot K_{\text{safety}}+1}\tag{64}$$

The CAV objective function is corrected in real time according to the corrected weight value. The model at this time is M2.

5 Experimental results

5.1 Experimental parameter settings

The data sources for the prediction and planning modules were derived from the ubiquitous traffic eye dataset. The experiments were conducted on a laptop with an Intel(R) Core i9–12900H processor (20 cores), 16 GB of RAM, a 512 GB NVMe SSD, and an NVIDIA GeForce RTX 3060 GPU running Windows 10 Pro. The software environment included Python 3.8.10, with key libraries such as PyTorch 1.8.0, TorchGeometric 1.7.0, NumPy 1.19.5, and Matplotlib 3.3.4, all developed via PyCharm Professional 2021.1. The experimental parameters were set on the basis of existing research findings and relevant industry standards, ensuring that the experimental results accurately reflected real-world conditions (Table 3).

For X1, the data features include the horizontal and vertical coordinates, speeds, and accelerations of two interacting vehicles. We utilized trajectory data from the Ubiquitous Traffic Eyes dataset, which contains a total of 1,043,910 entries. From this dataset, we filtered out 88,909 trajectories involving interactions between two vehicles. Moving on to X2, the data features expand to include the mean and standard deviation of the D-SVO, along with the coordinates, speeds, and accelerations of the two interacting vehicles. Similarly, 88,909 interaction trajectories were

Table 3 Settings of the experimental parameters

Parameter	Value	Explanation
Δt	0.1	Update frequency (s)
T_{max}, T_{min}	4.0, 5.0	Planning duration (s)
c_{max}	1.0	Maximum curvature (m^{-1})
$v_{max\text{-}lon}$, $v_{min\text{-}lon}$	50, 3.0	Maximum and minimum longitudinal speed ($m{\cdot}s^{-1}$)
$a_{max\text{-}lon}$, $a_{min\text{-}lon}$	3.0, −3.0	Maximum and minimum longitudinal acceleration ($m{\cdot}s^{-2}$)
$v_{max\text{-}lat}$, $v_{min\text{-}lat}$	2.0, 0.0	Maximum and minimum lateral speed ($m{\cdot}s^{-1}$)
$a_{max\text{-}lat}$, $a_{min\text{-}lat}$	2.0, −2.0	Maximum and minimum lateral acceleration ($m{\cdot}s^{-2}$)
K_{safety}, $K_{comfort}$, $K_{efficiency}$, $K_{consistency}$	0.25, 0.25, 0.25, 0.25	Initial weights for cost function

selected from the Ubiquitous Traffic Eyes dataset, with the mean and standard deviation of the SVO estimated via an algorithm based on literature. For X3, the dataset incorporates the horizontal and vertical coordinates, speeds, and accelerations of the two interacting vehicles, as well as the safety loss and consistency loss values for all candidate trajectories of the CAV. This subset also consists of 88,909 trajectories. In the cases of X4 and X5, the data features include not only the coordinates, speeds, accelerations, safety loss, and consistency loss values of the interacting vehicles and CAV candidate trajectories but also the mean and standard deviation of the D-SVO. Both X4 and X5 share the same dataset of 88,909 interaction trajectories. A summary of the data samples for the different models is provided in Table 4.

For the prediction model, optimal performance across all the prediction modules was achieved via the grid-search method. The learning rate was varied between 0.0001, 0.001, and 0.01, while the batch size was set to 16, 32, and 64. Additionally, the number of epochs was adjusted to 50, 100, and 150. The details of these parameter settings are presented in Table 5.

The other parameters are shown in Table 6.

Table 4 Data samples X1, X2, X3, X4, and X5

(a) Data sample of X1

Frame	Time	Car1	Land1	x_1	y_1	v_1	a_1	Car2	Land2	x_2	y_2	v_2	a_2
5,251	87.51	102	2	5.03	−0.18	15.59	1.65	104	1	5.93	1.05	12.14	0.82
5,252	87.53	102	2	5.17	−0.18	16.00	0.55	104	1	6.00	1.05	12.42	0.54
—	—	—	—	—	—	—	—	—	—	—	—	—	—

(b) Data sample of X2

Frame	Time	Car1	Land1	x_1	y_1	v_1	a_1
5,251	87.51	102	2	5.03	−0.18	15.59	1.65
5,252	87.53	102	2	5.17	−0.18	16.00	0.55
—	—	—	—	—	—	—	—

Frame	Time	Car2	Land2	x_2	y_2	v_2	a_2	SVO	SVO-std
5,251	87.51	104	1	5.93	1.05	12.14	0.82	46.88	1.14
5,252	87.53	104	1	6.00	1.05	12.42	0.54	46.26	1.11
—	—	—	—	—	—	—	—	—	—

(c) Data sample for X3

Frame	Time	Car1	Land1	x_1	y_1	v_1	a_1	Car2	Land2	x_2	y_2	v_2	a_2
5,251	87.51	102	2	5.03	−0.18	15.59	1.65	104	1	5.93	1.05	12.14	0.82
5,252	87.53	102	2	5.17	−0.18	16.00	0.55	104	1	6.00	1.05	12.42	0.54
—	—	—	—	—	—	—	—	—	—	—	—	—	—

Safety 1	Consistency 1	Safety 2	Consistency 2	Safety 3	Consistency 3	…	…
0.15	0.12	0.18	0.12	0.25	0.20	—	—
0.35	0.44	0.31	0.42	0.50	0.61	—	—
—	—	—	—	—	—	—	—

(d) Data sample for X4 and X5

Frame	Time	Car1	Land1	x_1	y_1	v_1	a_1	Car2	Land2	x_2	y_2	v_2	a_2
5,251	87.51	102	2	5.03	−0.18	15.59	1.65	104	1	5.93	1.05	12.14	0.82
5,252	87.53	102	2	5.17	−0.18	16.00	0.55	104	1	6.00	1.05	12.42	0.54
—	—	—	—	—	—	—	—	—	—	—	—	—	—

Safety 1	Consistency 1	Safety 2	Consistency 2	…	…	SVO	SVO-std
0.15	0.12	0.18	0.12	—	—	46.88	1.14
0.35	0.44	0.31	0.42	—	—	46.26	1.11
—	—	—	—	—	—	—	—

Table 5 Hyperparameter settings

Prediction model	Learning rate	Batch size	Epoch
F1	0.001	64	50
F2	0.001	64	50
F3	0.0001	64	100
F4	0.001	64	50
F5	0.0001	32	100

Table 6 Other parameters for the prediction module

Parameter	Value	Parameter	Value
Sliding window	30	Hidden layer	256
LSTM layer	2	Dropout rate	0.05

This study proposes a joint prediction-planning algorithm for CAVs based on SVO and conducts corresponding evaluations on three innovative points, including optimization analysis of trajectories by improving the objective function and optimization analysis of trajectories by SVO and optimization analysis of trajectories by joint predictive planning.

X1 is a combination of F1 and M1, X2 is a combination of F2 and M2, X3 is a combination of F3 and M1, and X4 is a combination of F4 and M2. X5 is a combination of F5 and M2.

5.2 Result analysis of trajectory by improving the objective function

This study first evaluates the optimization effect of the improved objective function on the trajectory. The purpose of the autonomous driving objective function is to select a safe and comfortable future trajectory, so it is crucial to be able to continuously output a stable and safe future trajectory. We choose the changes in the safety potential energy field strength and acceleration to illustrate the performance of the algorithm in terms of safety and comfort, respectively. The models used in the comparison are M2, M2.1 (considering only the consistency function), M2.2 (considering only the HDV's SVO), and M2.3 (not considering the consistency function and HDV's SVO).

As shown in Table 7, among all the algorithms, the mean value and standard deviation of the CAV safety potential energy field strength under M2 are only 0.1683, and the standard deviation is 0.0591. The mean and standard deviation of the CAV safety potential energy field strength under M2.3 reach 0.3129 and 0.3139, respectively. Although the performance of M2.2 and M2.1 is worse than that of M2.3, it is still not as good as the performance of M2. Second, as shown in Fig. 3, the distribution of the safety potential energy field strength under M2 is relatively concentrated without any abnormal values, whereas M2.1, M2.2, and M2.3 all have abnormal values to varying degrees. Therefore, the following conclusions are drawn:

1) **Stability and Safety Enhancement:** Integrating SVO and the consistency function into the objective function significantly improves the stability and safety of CAV trajectories, as evidenced by the lower mean and standard deviation in the safety potential energy field and the absence of abnormal values in M2.

2) **Importance of comprehensive integration:** While individual consideration of SVO or the consistency function provides some benefits, the combination of both, as in M2, yields the best performance, ensuring that CAVs operate within a safer, more stable risk environment, thus enhancing overall safety and comfort.

Table 7 Standard deviation and average value of the safe potential energy field

	M2	M2.1	M2.2	M2.3
Std	**0.0591**	0.1368	0.2005	0.3139
Mean	**0.1683**	0.2092	0.2303	0.3129

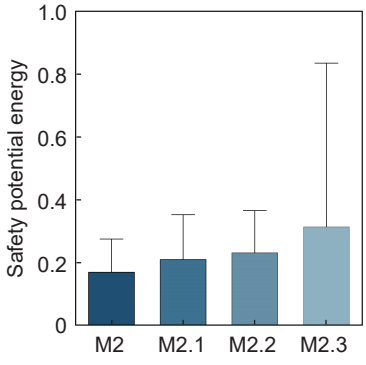

Fig. 3 CAV safety potential energy field distribution diagram.

5.3 Result analysis of trajectory based on SVO

This section mainly evaluates the impact of SVO on CAV joint forecast planning results. The ideal optimal trajectory is the comparison benchmark under the same situation, which is used to evaluate the relative error between the output trajectories of X1, X2, and X3. FDE and MR are used as evaluation indicators. These three indicators are important reference indicators in the field of trajectory prediction research and have important guiding significance for the evaluation of the experimental results of this study. The evaluation content includes two parts. The first is the analysis of results under continuous experiments and the analysis of results under different SVOs.

CAV joint prediction planning has a certain degree of randomness. To fully evaluate the optimization effect of SVO on the CAV output trajectory, we conducted 30 consecutive experiments, as shown in Figs. 4 and 5 and Table 8. Overall, the average ADEs of X1 and X2 are 6.633 and 5.847 m, respectively, and the average FDEs are 3.329 and 2.151 m, respectively. The average ADEs of X3 and X4 are 5.660 and 4.213 m, respectively, and the average FDEs are 2.545 and 2.051 m, respectively. Therefore, the following conclusions are drawn.

1) **Impact of SVO on trajectory accuracy**: The inclusion of SVO significantly reduces both ADE and FDE, as demonstrated by the improved performance of X3 and X4 over X1 and X2. This finding indicates that models accounting for social dynamics are better at predicting more accurate and reliable trajectories, aligning closer to the ideal optimal trajectory.

2) **Consistency in performance across experiments**: The 30

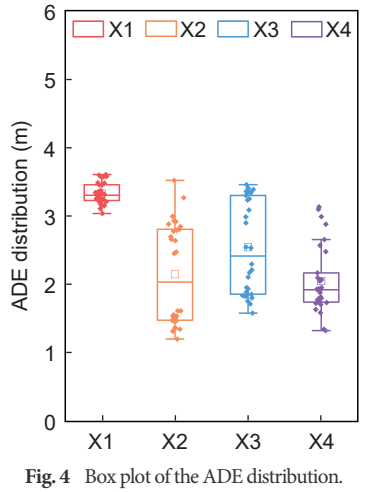

Fig. 4 Box plot of the ADE distribution.

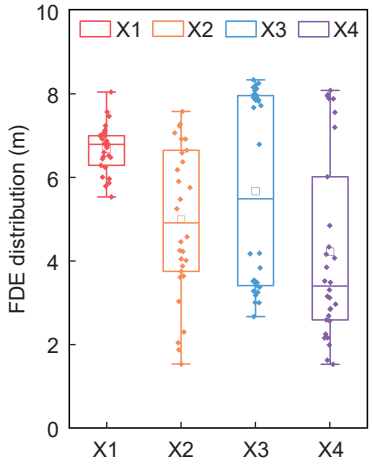

Fig. 5 FDE distribution box plot.

Table 8 Results distribution table of the ADE and FDE methods.

	ADE			FDE		
	Max	Min	Mean	Max	Min	Mean
X1	3.606	3.038	3.329	8.030	5.523	6.633
X2	**3.521**	**1.203**	**2.151**	**7.565**	**1.528**	**5.847**
X3	3.459	1.582	2.545	8.323	2.662	5.660
X4	**3.134**	**1.327**	**2.051**	**8.071**	**1.523**	**4.213**

consecutive experiments reveal that integrating SVO leads to more consistent and predictable outputs, with lower variations in key metrics such as ADE and FDE. This consistency underscores the importance of considering social factors in the joint prediction planning process, as it enhances the robustness of CAVs' decision-making under various scenarios, ultimately leading to safer and more reliable autonomous driving outcomes.

As shown in Figs. 6 and 7, the ADE of X2 is smaller than that of X1, and the ADE of X4 is smaller than that of X3. Moreover, the FDE of X2 is smaller than that of X1, and the FDE of X4 is smaller than that of X3.

As shown in Fig. 8, we further draw the ADE error band charts of X1–X4 and the trajectory charts of X1–X4. In the same experimental scenario, compared with the comparison model (X1 and X3), the output trajectories of SVO (X2 and X4) fit the ideal trajectory better, with smaller errors. Therefore, in the CAV prediction planning model considering SVO, whether the prediction target is the future trajectory of the HDV or the direct prediction of the CAV's loss value distribution can improve the reliability of the CAV's output trajectory to a certain extent. The

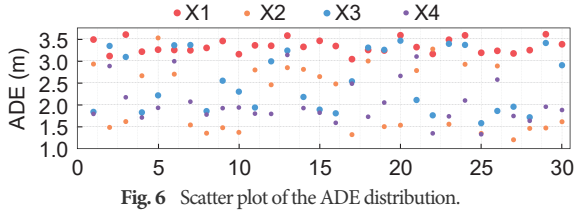

Fig. 6 Scatter plot of the ADE distribution.

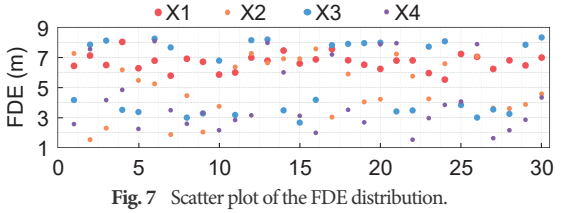

Fig. 7 Scatter plot of the FDE distribution.

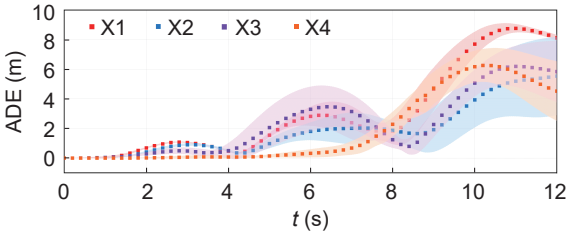

Fig. 8 ADE error bands of X1-X4.

conclusion is that incorporating SVO into the CAV prediction planning model significantly improves trajectory accuracy, ensuring better alignment with the ideal path and enhancing the overall reliability of autonomous driving systems.

5.4 Result analysis of trajectory through joint prediction and planning

This section aims to evaluate the impact of the intelligent "prediction-optimization" method on the results of CAV joint prediction and planning. Using the ideal optimal trajectory under the same conditions as the comparative benchmark, we assess the relative errors between the output trajectories of X2, X4, and X5 and the ideal trajectory under the same scenario. ADE, FDE, and MR are used as evaluation metrics. These three metrics are important references in the field of trajectory prediction research and have guiding significance for the evaluation of the experimental results in this paper. The evaluation includes two parts: the first is the analysis of results under continuous random experiments, and the second is the analysis of results under different sensitive parameters.

We conducted ten consecutive random experiments, in which the HDV randomly fluctuated within the allowable range, but the numerical value of each change was identical across different model tests. The distribution of ADEs is illustrated in Fig. 9. First, the average ADE of X5 ranged from a minimum of 0.52 m to a maximum of 4.03 m, which was significantly lower than the output results of X2 and X4 under the same conditions. Additionally, the minimum standard deviation of X5 was 0.78 m, and the maximum was 3.17 m, whereas the minimum standard deviation of X2 reached 2.07 m, and the maximum was 4.56 m. The minimum standard deviation of X4 reached 1.35 m, and the maximum was 4.45 m. Therefore, the conclusions are shown below.

Enhanced accuracy and consistency: The smart "prediction-optimization" method in Model X5 significantly outperforms X2 and X4, resulting in a lower ADE and standard deviation, which leads to more accurate and consistent trajectory predictions.

Improved stability: X5's consistent performance across random experiments demonstrates the robustness of the "prediction-optimization" approach, effectively handling HDV fluctuations and resulting in more stable and reliable CAV trajectory planning.

As shown in Fig. 10, we further evaluated the MR. In the 10 consecutive random experiments, the MR of X5 was no less than 50%, which was higher than the maximum MR of X2 and X4.

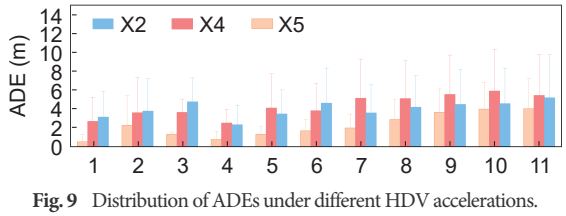

Fig. 9 Distribution of ADEs under different HDV accelerations.

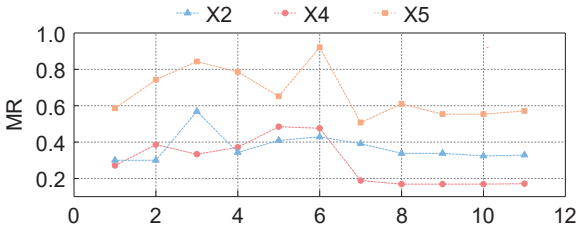

Fig. 10 Distribution of MR under different HDV accelerations.

Additionally, X5 achieved six results above 60% and two results above 80%. Under the same conditions, the MR of X2 did not exceed 60%, and the MR of X4 did not exceed 40%. Moreover, the majority of the MR distributions for both X2 and X4 fell within the range of [20%, 40%]. Therefore, we conclude that the CAV joint prediction and planning model that considers Smart Predict-Optimize (SPO) can effectively meet planning requirements, resulting in a lower deviation and better fit between the output trajectory and the ideal trajectory.

The time domain and update frequency for CAV trajectory planning are crucial sensitivity parameters in joint prediction planning. A smaller time domain and lower frequency may cause the CAV to overlook some traffic elements in the road scene, compromising safety while reducing the computational load. Conversely, a larger time domain and higher frequency may improve safety but increase the computational load. On the basis of existing research, we set the planning time domain to 4.5, 5.0, and 5.5 s and the update frequency to 0.1, 0.2, and 0.3 s, resulting in nine combinations of sensitivity parameters. We used the ADE, FDE, and MR as evaluation metrics. As shown in Tables 9–11, the ADE of X5 is consistently lower than that of X2 and X4. Additionally, within the same time domain, the ADE of X5 gradually decreases as the frequency increases. For example, when the time domain is 4.5 s, the ADEs are 2.24, 1.82, and 1.51 m, respectively. However, when the frequency is 0.1 s, the ADE of X5 first decreases and then increases as the time domain increases. Conversely, when the frequency is 0.2 and 0.3 s, the ADE of X5 continues to decrease as the time domain increases. This may be because, under certain update frequencies, a higher time domain allows the CAV to consider more traffic elements ahead, resulting in differences between the output trajectory of the CAV and that of shorter time domains. Similarly, the performance of X5 in terms of FDE and MR is superior to that of X2 and X4 under the same conditions. The results demonstrate that the CAV joint prediction-planning model incorporating the smart "prediction-optimization" method (X5) exhibits strong adaptability and consistently superior performance across various time domains and update frequency settings, making it more reliable and effective than models X2 and X4 under diverse conditions.

Table 9 ADE under different sensitivity parameter settings

T (s)	Δt (s)	X5	X4	X2
		ADE (m)	ADE (m)	ADE (m)
4.5	0.1	**2.24**	6.75	3.92
	0.2	**1.82**	3.58	2.56
	0.3	**1.51**	1.92	1.81
5.0	0.1	**1.81**	5.93	2.10
	0.2	**1.32**	3.22	2.54
	0.3	**0.98**	2.10	1.71
5.5	0.1	**2.01**	6.41	2.35
	0.2	**1.14**	3.48	2.35
	0.3	**0.66**	2.02	1.75

Table 10 FDE under different sensitivity parameter settings

T (s)	Δt (s)	X5	X4	X2
		FDE (m)	FDE (m)	FDE (m)
4.5	0.1	**2.66**	18.01	11.10
	0.2	**0.54**	9.00	7.14
	0.3	**4.17**	4.59	4.52
5.0	0.1	**3.16**	16.32	5.23
	0.2	**6.52**	10.87	7.32
	0.3	**1.07**	4.79	5.01
5.5	0.1	**3.68**	17.68	5.85
	0.2	**4.62**	10.71	6.25
	0.3	**0.57**	5.21	5.16

Table 11 MR under different sensitivity parameter settings

T (s)	Δt (s)	X5	X4	X2
		MR (%)	MR (%)	MR (%)
4.5	0.1	**58.33**	24.17	41.67
	0.2	**50.00**	25.00	48.33
	0.3	**66.67**	40.00	60.00
5.0	0.1	**66.37**	34.51	48.67
	0.2	**85.24**	45.90	50.82
	0.3	**92.31**	43.59	64.10
5.5	0.1	**50.00**	30.00	47.27
	0.2	**86.88**	40.98	52.46
	0.3	**100.00**	51.28	61.54

Furthermore, we analyze the phenomenon from the perspective of individual distribution. As shown in Fig. 11, the results indicate that the joint prediction planning of CAVs under SPO can achieve superior accuracy and trajectory stability, further supporting the conclusions mentioned above.

6 Conclusions

This study proposes three models. M2 refers to the CAV planning algorithm based on HDV future trajectory data and D-SVO. X2 takes "HDV trajectory data, CAV trajectory data, and D-SVO" as input and predicts the future trajectory of the HDV (F2) with the objective of minimizing the weighted sum of the HDV prediction trajectory error and D-SVO prediction error. The predicted HDV trajectory is then input into M2 to output the optimal trajectory. X4 takes "HDV trajectory data, CAV trajectory data, CAV loss values, and D-SVO" as input and predicts the future loss value of CAVs (F4) with the objective of minimizing the weighted sum of the predicted CAV future loss value and D-SVO prediction error. The loss value is then input into M2 to output the optimal trajectory. The X5 (F5+M2) model implements the logic of "intelligent prediction-optimization". X5 takes "HDV trajectory data, CAV trajectory data, CAV loss values, and D-SVO" as input and constructs an AIF in the prediction model by considering the optimization objective and D-SVO. The AIF is used as the

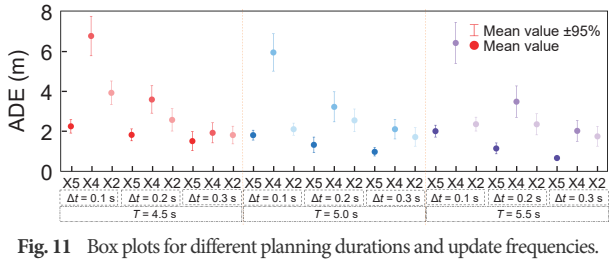

Fig. 11 Box plots for different planning durations and update frequencies.

objective to predict the future loss value of CAV (F5), and the loss value is then input into M2 to output the optimal trajectory. The experimental results show that the joint prediction and planning of CAVs considering the SVO and SPO exhibit excellent performance in terms of trajectory output accuracy, stability, and adaptability. This enables CAVs to effectively adapt to the influence of other HDVs in mixed traffic flows and make more reliable decision-making and planning. For future research, on the basis of the results of this study, we will shift the planning algorithm from single-vehicle intelligent planning to multivehicle collaborative planning and propose a joint prediction-planning framework for multivehicle collaboration on the basis of SVO, realizing the possibility of large-scale application of autonomous driving technology. In today's mixed traffic environments, where HDVs and autonomous vehicles coexist, social interactions between different vehicles have become increasingly common. As you mentioned, traditional pipeline technologies struggle to manage all corner cases, potentially leading to severe accidents. End-to-end approaches, however, can reduce information loss across different modules, such as perception, prediction, planning, and control. Thus, a promising research direction is the development of an "Integrated Interaction-Optimized Architecture for Autonomous Vehicle Prediction and Planning" to enhance social interaction capabilities and minimize information loss for autonomous vehicles in the near future.

Appendix

Behavioral and experimental economics show that drivers exhibit unique social decision-making preferences, such as altruism, fairness, reciprocity, aversion to inequity, and egalitarianism. The assumption that drivers make decisions solely on the basis of individual needs overlooks the variability in how different driver groups behave across various scenarios. SVO addresses this by capturing a driver's preferences for how rewards are distributed between themselves and others. SVO can predict behaviors such as cooperative motivation, negotiation strategies, and decision-making processes. For CAVs, understanding the SVO of human drivers can significantly enhance behavior prediction, particularly in situations that require cooperation, such as navigating intersections. Without considering SVO, an AV might adopt a more conservative approach, waiting for all HDVs to pass before proceeding. Since drivers do not directly communicate their SVO, AVs must infer it on the basis of observed behaviors and social cues. We estimate a driver's SVO by identifying which SVO most closely aligns with their predicted and actual driving trajectories. This method enables us to infer the SVO distribution within a population of drivers, beyond specific driving scenarios. SVO, a concept from psychology, refers to individuals' preferences for distributing outcomes between themselves and others in interdependent situations, influencing behavior in social dilemmas. It is primarily categorized into prosocial and proself types. When applied to road traffic, social dilemmas involve interactions between vehicles, where SVO affects decision-making.

In traditional traffic flow, social interaction occurs mainly among HDVs, and this interaction is realized through acceleration, deceleration, horns, lane changes, flashlights, and other methods. SVO's angle is assumed to range from 0° to 90°, with a completely prosocial driver having an angle of 90° and a completely proself driver having an angle of 0°. Studies have shown that prosocial drivers tend to have cooperative intentions, which means that they achieve driving consistency with interacting vehicles through decision-making control. Proself drivers tend to pursue the maximization of benefits, where benefits may include the maximization of driving space and the minimization of driving time, academically known as the maximization of space occupancy and time occupancy. Therefore, prosocial drivers and prosocial drivers can achieve their goals through cooperation, showing the strongest sense of cooperation; prosocial drivers and proself drivers present a one-sided trend, with the former seeking reasonable decision-making space while driving and the latter seeking any possible decision-making space; proself drivers and proself drivers pursue selfish driving benefit maximization in the game of competition.

When CAVs have no knowledge of the characteristics of HDV drivers, CAVs need to estimate the drivers' SVO. We can evaluate it through the relative states between CAVs and HDVs. The first factor is speed. Proself drivers seek to maximize their dynamic space occupancy and dynamic time occupancy on the road, which is most directly reflected in the relative speed between CAVs and HDVs. The advantage of SVO lies in its ability to quantify drivers' social preferences for allocating resources to themselves and others in specific situations. If the speed of the HDV is equal to that of the CAV, we can consider the SVO to be 45°; if the HDV speed is greater than the CAV speed, the HDV expects to seek safer, more comfortable, and efficient driving space through higher speeds during the interaction, indicating a weaker willingness for cooperation and fair decision-making and a SVO tending toward 0°. If the HDV speed is lower than the CAV speed, the HDV is more inclined to achieve vehicle driving through reasonable decision-making during the interaction, with a stronger willingness for cooperation and a SVO tending toward 90°. The second factor is acceleration and jerk. Proself drivers seek greater driving benefits and respond to various potential risks through frequent acceleration and deceleration behaviors, resulting in larger absolute values of acceleration and jerk. In contrast, prosocial drivers achieve safety and comfort through stable driving, with lower absolute values of acceleration and jerk. Therefore, we can construct an estimation value of the driver's SVO by using the speed comparison as the base, acceleration and jerk as the exponent, and 45° as the constant.

$$\text{D-SVO}^{\circ} = \left(\frac{v_{\text{cav}}}{v_{\text{hdv}}}\right)^{\mu_1\left|\frac{a_{\text{hdv}}}{a_{\max}}\right|+\mu_2\left|\frac{j_{\text{hdv}}}{j_{\max}}\right|} \cdot \text{D-SVO}^{\circ}_{\max/2},$$
$$0^{\circ} \leqslant \text{D-SVO}^{\circ} \leqslant 90^{\circ} \tag{A1}$$

Furthermore, the estimated value of SVO provides a baseline for HDV drivers, allowing us to further construct a standard deviation of SVO and establish a Gaussian distribution model for SVO. Imagine a scenario where the distance between a CAV and an HDV is considerable and where there is virtually no interaction between them. In such a case, the accuracy of the abovementioned estimation of the HDV driver's SVO would decrease, and the impact of SVO on the decision-making and planning of the CAV would also diminish. As the CAV approaches the HV, the social interaction or game-playing phenomenon between them becomes more apparent, making both the SVO estimation and its influence on the CAV more reliable. Therefore, it is necessary to introduce an indicator to illustrate the degree of interaction between the CAV and the HDV, namely, the safety potential field. The safety potential field takes into account the trajectory data of both the CAV and the HDV to derive the safety potential field generated by the HDV at the location of the CAV. A higher value of the safety potential field indicates a greater degree of interaction between the CAV and the HDV, and vice versa.

$$\text{D-SVO}^{\circ}_{\text{std}} \leftarrow \left| \frac{\boldsymbol{E}_{\max}}{\boldsymbol{E}_{\text{hdv}\rightarrow\text{cav}}} \right| \cdot \text{D-SVO}^{\circ}_{\max/4} \quad \text{(A2)}$$

Therefore, we constructed a Gaussian distribution model to represent the D-SVO of HDV drivers. The estimated value of SVO reflects the overall trend in how HDV drivers allocate driving benefits, whereas the standard deviation of SVO indicates the degree of trust that CAVs have in their estimations of HDV drivers' SVO. We illustrate this via data from the Ubiquitous Traffic Eyes (Figs. A1–A5).

As shown in Figs. A1 and A3, the SVO of Vehicle 1 and Vehicle 2 is represented, illustrating how each vehicle balances its self-interest with the interests of others. A higher SVO, indicating more prosocial behavior, leads to greater consideration of the welfare of surrounding vehicles. As the SVO of Vehicle 1 increases (demonstrating more prosocial behavior), its safety potential field remains lower, meaning that Vehicle 1 takes fewer risks and acts more cooperatively. In contrast, when Vehicle 2 has a lower SVO (indicating more individualistic behavior), its safety potential field fluctuates more, suggesting a higher tolerance for risk and less cooperative behavior. The alignment between SVO and the safety potential field helps explain why one vehicle may yield more frequently than the other to avoid collisions.

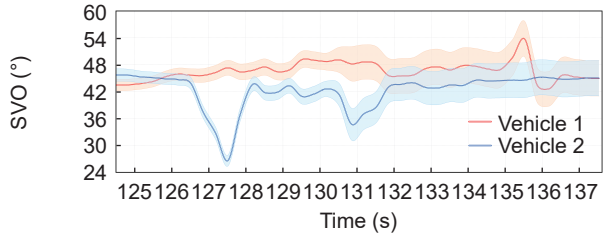

Fig. A1 Distribution of drivers' SVO under naturalistic driving data.

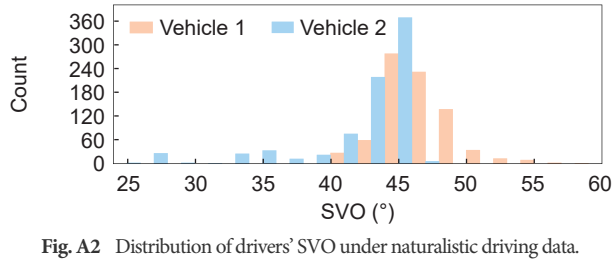

Fig. A2 Distribution of drivers' SVO under naturalistic driving data.

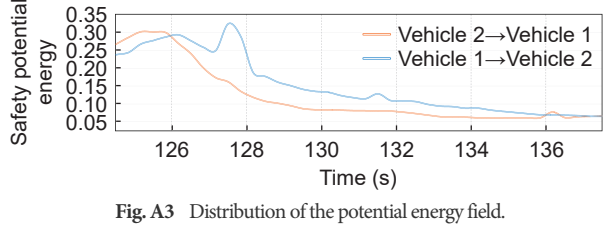

Fig. A3 Distribution of the potential energy field.

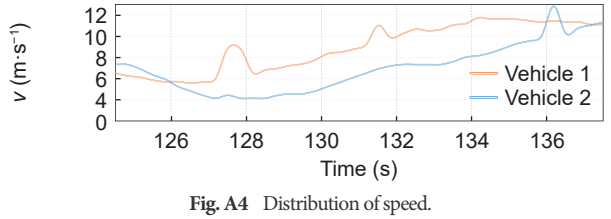

Fig. A4 Distribution of speed.

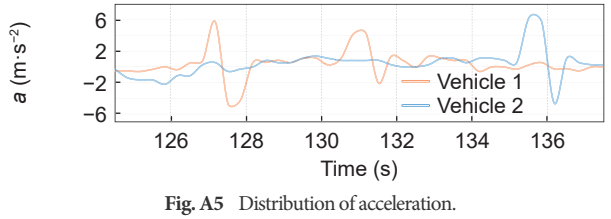

Fig. A5 Distribution of acceleration.

The speed profiles of Vehicle 1 and Vehicle 2 are presented in Figs. A1 and A4. Drivers with a higher SVO, indicating more prosocial behavior, tend to adjust their speed in response to surrounding vehicles to avoid conflicts, especially in situations such as merging or lane changes. The speed profile of Vehicle 1, which has a higher SVO, shows smoother adjustments with fewer spikes, suggesting that Vehicle 1 adapts its speed to maintain safe distances and promote cooperative driving behavior. In contrast, Vehicle 2, with a lower SVO, exhibits more abrupt changes in speed, reflecting more aggressive or individualistic driving. This indicates that Vehicle 2 may prioritize its own objectives (e.g., getting ahead) over the safety of others, leading to more erratic speed variations.

As shown in Figs. A1 and A5, acceleration directly reflects how a vehicle adjusts its speed over time, offering insight into a driver's decision-making process in traffic. Vehicle 1, with a higher SVO, displays more controlled and consistent acceleration, indicating a cautious and cooperative approach. This behavior aligns with prosocial decision-making, where the driver avoids sudden acceleration that might cause discomfort or pose risks to others. In contrast, Vehicle 2 exhibits sharper changes in acceleration, particularly in situations where cooperation is less prioritized. This suggests that Vehicle 2 behaves more competitively or independently, potentially making abrupt decisions without considering the collective safety of the surrounding environment.

Higher SVO (more prosocial): Vehicle 1 shows a greater tendency for cooperative driving, reflected in a smoother safety potential field, controlled speed, and steady acceleration. This indicates a safer and more predictable driving pattern.

Lower SVO (more individualistic): Vehicle 2, by contrast, takes more risks, as shown by its fluctuating safety potential field, erratic speed, and abrupt acceleration. This behavior suggests more competitive and self-focused driving tendencies, with less regard for the surrounding vehicles.

Replication and data sharing

The Python program code used within this research can be made accessible upon request via email to the corresponding author.

Acknowledgements

This study was supported by the Science and Technology Plan of Zhejiang Provincial Department of Transportation (Grant No. 2024017), the "Pioneer" and "Leading Goose" R&D Program of Zhejiang (Grant No. 2022C01050), the Fundamental Research Funds for the Central Universities (Grant No. 2024BSSXM01), the National Natural Science Foundation of China (Grant No. 72361137006), the Natural Science Foundation of Zhejiang Province (Grant No. LR23E080002), the Research Project of Balanced Building Research Center, Zhejiang University (Grant No. K20212792), and the Research Grants Council of the Hong Kong Special Administrative Region, China (Grant No. 15210620).

Declaration of competing interest

The authors have no competing interests to declare that are relevant to the content of this article.

References

Altche, F., Polack, P., de la Fortelle, A., 2017. High-speed trajectory planning for autonomous vehicles using a simple dynamic model. In: 2017 IEEE 20th International Conference on Intelligent Transportation Systems (ITSC), 1–7.

Bai, C., Jin, S., Jing, J., Yang, C., Yao, W., Rong, D., et al., 2024. A multimodal data-driven approach for driving risk assessment. *Transp Res Part E Logist Transp Rev*, **189**, 103678.

Cai, P., He, J., Li, Y., 2023. Hybrid cooperative intersection management for connected automated vehicles and pedestrians. *J Intel Connect Veh*, **6**, 91–101.

Chen, Y., Veer, S., Karkus, P., Pavone, M., 2023. Interactive joint planning for autonomous vehicles. *IEEE Robot Autom Lett*, **9**, 987–994.

Dai, C., Zong, C., Zhang, D., Li, G., Chuyo, K., Zheng, H., et al., 2023. Human-like lane-changing trajectory planning algorithm for human-machine conflict mitigation. *J Intel Connect Veh*, **6**, 46–63.

Dixit, S., Montanaro, U., Fallah, S., Dianati, M., Oxtoby, D., Mizutani, T., et al., 2018. Trajectory planning for autonomous high-speed overtaking using MPC with terminal set constraints. In: 2018 21st International Conference on Intelligent Transportation Systems (ITSC), 1061–1068.

Hubmann, C., Becker, M., Althoff, D., Lenz, D., Stiller, C., 2017. Decision making for autonomous driving considering interaction and uncertain prediction of surrounding vehicles. In: 2017 IEEE Intelligent Vehicles Symposium (IV), 1671–1678.

Jeon, J. H., Cowlagi, R. V., Peters, S. C., Karaman, S., Frazzoli, E., Tsiotras, P., et al., 2013. Optimal motion planning with the half-car dynamical model for autonomous high-speed driving. In: 2013 American Control Conference, 188–193.

Jiang, K., Zhou, Y., 2021. Optimization of vehicle trajectory planning for autonomous high-speed overtaking. In: 2021 IEEE 4th International Conference on Automation, Electronics and Electrical Engineering (AUTEEE), 9–13.

Liu, K., Gong, J., Kurt, A., Chen, H., Ozguner, U., 2018. Dynamic modeling and control of high-speed automated vehicles for lane change maneuver. *IEEE Trans Intell Veh*, **3**, 329–339.

Michael, W. L., Stephen, D. B., 2016. A cell transmission model for dynamic lane reversal with autonomous vehicles. *Transp Res Part C Emerg Technol*, **68**, 126–143.

Mo, X., Lv, C., 2023. Predictive neural motion planner for autonomous driving using graph networks. *IEEE Trans Intell Veh*, **8**, 1983–1993.

Qiu, J., Du, L., 2023. Cooperative trajectory control for synchronizing the movement of two connected and autonomous vehicles separated in a mixed traffic flow. *Transp Res Part B Methodol*, **174**, 102769.

Richter, C., Ware, J., Roy, N., 2014. High-speed autonomous navigation of unknown environments using learned probabilities of collision. In: 2014 IEEE International Conference on Robotics and Automation (ICRA), 6114–6121.

Rong, D., Jin, S., Yao, W., Yang, C., Bai, C., Alagbé, A. J., 2024a. Hybrid trajectory planning for connected and autonomous vehicle considering communication spoofing attacks. *IEEE Trans Intell Transp Syst*, **25**, 11961–11976.

Rong, D., Jin, S., Xu, M., Yao, W., Yang, C., Bai, C., et al., 2024b. Integration of multi-vehicle prediction and planning based on social value orientation in mixed traffic. https://doi.org/10.1109/TIV.2024.3442214

Sazgar, H., Azadi, S., Kazemi, R., 2018. Trajectory planning and integrated control with the nonlinear bicycle model for high-speed autonomous lane change. *Modares Mech Eng*, **18**, 103–114.

Tomas-Gabarron, J. B., Egea-Lopez, E., Garcia-Haro, J., 2013. Vehicular trajectory optimization for cooperative collision avoidance at high speeds. *IEEE Trans Intell Transp Syst*, **14**, 1930–1941.

Wang, W., Zhang, Y., Gao, J., Jiang, Y., Yang, Y., Zheng, Z., et al., 2023. GOPS: A general optimal control problem solver for autonomous driving and industrial control applications. *Commun Transp Res*, **3**, 100096.

Wang, Y., Li, S., Cheng, W., Cui, X., Su, B., 2020. Toward efficient trajectory planning based on deterministic sampling and optimization. In: 2020 Chinese Automation Congress (CAC), 1318–1323.

Yan, Y., Peng, L., Shen, T., Wang, J., Pi, D., Cao, D., et al., 2023. A multi-vehicle game-theoretic framework for decision making and planning of autonomous vehicles in mixed traffic. *IEEE Trans Intell Veh*, **8**, 4572–4587.

Yu, Y., Luo, X., Su, Q., Peng, W., 2023. A dynamic lane-changing decision and trajectory planning model of autonomous vehicles under mixed autonomous vehicle and human-driven vehicle environment. *Phys A Stat Mech Appl*, **609**, 128361.

Zhang, E., Zhang, R., Masoud, N., 2023. Predictive trajectory planning for autonomous vehicles at intersections using reinforcement learning. *Transp Res Part C Emerg Technol*, **149**, 104063.

Zhou, D., Ma, Z., Sun, J., 2019. Autonomous vehicles' turning motion planning for conflict areas at mixed-flow intersections. *IEEE Trans Intell Veh*, **5**, 204–216.

Zhou, J., Olofsson, B., Frisk, E., 2023. Interaction-aware motion planning for autonomous vehicles with multi-modal obstacle uncertainty predictions. *IEEE Trans Intell Veh*, **9**, 1305–1319.

Dongelei Rong is currently a Ph.D. candidate in the Institute of Intelligent Transportation Systems, College of Civil Engineering and Architecture, Zhejiang University and The Hong Kong Polytechnic University. His research interests include intelligent transportation systems, autonomous vehicle, trajectory planning, and traffic modeling.

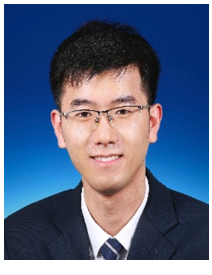

Yuefeng Wu is currently the chief engineer in Xinchang Communications Investment Group Co., Ltd., with extensive experience in transportation planning and construction management. As the project leader, he has served as the principal investigator for numerous significant projects.

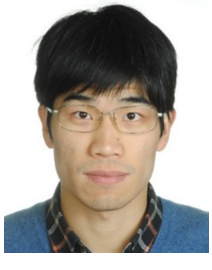

Wenjun Du is currently a senior engineer of transportation engineering in Zhejiang Institute of Communications Co., Ltd. His research interests include transportation consulting, planning, design, and intelligent transportation systems.

Chengcheng Yang received the B.S. degree from the School of Automotive and Traffic Engineering at Jiangsu University, Zhenjiang, China, in 2017; the M.S. degree from the School of management at the University of Shanghai for Science and Technology, Shanghai, China, in 2021. He is currently working toward the Ph.D. degree with Institute of Intelligent Transportation Systems of College of Civil Engineering and Architecture, Zhejiang University, Hangzhou, China. His research interest includes traffic flow theory and traffic control.

Sheng Jin received the Ph.D. degree in transportation engineering from Jilin University, Changchun, China, in 2010. Now, he is a professor with the College of Civil Engineering and Architecture, Zhejiang University, Hangzhou, China. He has published more than 80 articles in related journals such as *Transportation Research Part A: Policy and Practice*, *Transportation Research Part B: Methodological*, *Transportation Research Part C: Emerging Technologies*, *Transportation Research Part D: Transport and Environment*, *Accident Analysis & Prevention*, *IEEE Transactions on Intelligent Transportation Systems*, and *IEEE Intelligent Transportation Systems Magazine*. His research is focused on traffic flow theory, intelligent transportation systems, traffic signal control, and traffic big data.

Min Xu received the B.S. degree in hydraulic engineering and economics (double degree) from Tsinghua University and the Ph.D. degree in transportation engineering from the National University of Singapore, Singapore. She is currently an associate professor with the Department of Industrial and Systems Engineering, The Hong Kong Polytechnic University. Her research interests include modeling and optimization problems in urban transportation and logistics systems with emerging technologies. She serves on the editorial advisory board for *Transportation Research Part C: Emerging Technologies* and *Transportation Research Part E: Logistics and Transportation Review*.

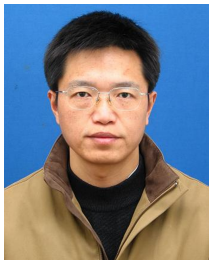

Fujian Wang received the M.S. and Ph.D. degrees in road engineering from Southeast University, China, in 1993 and 1996, respectively. From 1996 to 1999, he was a postdoctoral researcher at Beijing Jiaotong University, China. Currently, he is an associate professor at the College of Civil Engineering and Architectures, Zhejiang University, China. His research interests include traffic flow theory and intelligent transportation.